



Development of a Bioimpedance Based Human Machine Interface

Huang Yunfei

**A Thesis Submitted in Partial Fulfillment of the Requirements for the Degree of
Master of Engineering in Electrical Engineering
Prince of Songkla University**

2009

Copyright of Prince of Songkla University

Thesis Title Development of a Bioimpedance Based Human Machine Interface
Author Mr. Huang Yunfei
Major Program Electrical Engineering

Major Advisor:

.....
(Asst. Prof. Dr. Pornchai Phukpattaranont)

Examining Committee:

.....Chairperson
(Assoc. Prof. Dr. Montri Karnjanadecha)

.....
(Assoc. Prof. Booncharoen Wongkittisuksa)

.....
(Asst. Prof. Dr. Pornchai Phukpattaranont)

.....
(Dr. Chatchai Suppitaksakul)

The Graduate School, Prince of Songkla University, has approved this thesis as partial fulfillment of the requirements for the Master of Engineering Degree in Electrical Engineering.

.....
(Assoc. Prof. Dr. Kerkchai Thongnoo)

Dean of Graduate School

Thesis Title Development of a Bioimpedance Based Human Machine Interface
Author Mr. Huang Yunfei
Major Program Electrical Engineering
Academic Year 2009

ABSTRACT

The thesis presents the development of a bioimpedance based human machine interface for people with motor disabilities. The system can be used for the above elbow amputee or the lower extremities paralysis by C4 or C5 level spinal cord injury. We use three electrodes to measure two channels of bioimpedance from the trapezius muscle. Bioimpedance changes when there is a movement in the segment of trapezius muscle. We can classify six types of motions resulting in seven operation capabilities for wheelchair control based on six types of shoulder movements, i.e. left shoulder up, right shoulder up, and both shoulder up for short time and long time. Our system is composed of the modified Howland current bridge circuit, which supplies the 0.3 mA sinusoidal ac current to the measurement system at the frequency of 50 kHz. NI PCI-6250 DAQ board was adopted to collect the data and LabVIEW 8.2 was used to implement the signal processing and control system. Algorithms applied in the system are an automatic threshold value adjustment, which adapt its value to the measured signal. Overshoot detection is used to detect the unexpected large change of the signal to avoid the wrong operation. The proposed system was evaluated with its applications in simulated LED and wheelchair controls. Result shows that the interface based on bioimpedance are feasible and stable.

Keywords: bioimpedance, wheelchair, human machine interface

ACKNOWLEDGEMENT

First of all, this work is partially supported by NECTEC-PSU center of excellence for rehabilitation engineering and Faculty of Engineering, Prince of Songkla University.

I would like to extend my sincere gratitude to my supervisor, Asst. Prof. Dr. Pornchai Phukpattaranont, for his patience, encouragement, and professional instructions during my thesis writing. I am deeply grateful of his help in the completion of this thesis.

High tribute shall be paid to the internal committees Assoc. Prof. Dr. Montri Karnjanadecha, Assoc. Prof. Booncharoen Wongkittisuksa and Asst. Prof. Dr. Pornchai Phukpattaranont, also to the external committee Dr. Chatchai Suphapitaksakul. They have drawn out their precious time for my thesis.

Specially, I would like to thanks Asst. Prof. Sawit Tanthanuch for his kindness direction and help during the thesis working and daily life.

I feel grateful to all the teachers in Prince of Songkla University who once offered me valuable courses and advice during my study.

Great thanks should go to my friends who have put considerable time and effort into their comments on the draft. Especially thanks give to Tai Bandisak. He has put a lot of time on helping me prepare for the thesis examination.

Then, I am very precious the help from my friends, Mr. Wang Shenming, Mr. Xu shubing, Mr. Wang Xianwei and Mr. Fu Dongjin who have help me to test the interface as volunteers.

I feel grateful to all the staffs in Faculty of Engineering who have helped me.

Finally, I am indebted to my parents and cousin for their continuous support and encouragement.

Huang Yunfei

CONTENTS

Chapter 1.	Introduction.....	1
1.1.	Importance of research and problem statement	1
1.2.	Literature review	2
1.3.	Thesis objective	4
1.4.	Thesis scope	4
1.5.	Methodology	5
1.6.	Conclusion	6
Chapter 2.	Theory	7
2.1.	Human machine interface	7
2.2.	Bioimpedance signals	9
2.3.	Bioimpedance equivalent circuit.....	10
2.4.	The effective factor of bioimpedance	12
2.5.	Four electrodes method.....	13
2.6.	Conclusion	14
Chapter 3.	Hardware design	15
3.1.	System configuration	15
3.1.1	Current source.....	16
3.1.1.1	Current source design.....	16
3.1.1.2	General resistor property analysis.....	17
3.1.1.3	Current source performance analysis.....	18
3.1.2	Current source frequency selection.....	20
3.1.3	Monitoring electrodes	22
3.1.4	NI PCI 6250 DAQ device.....	23
3.2.	Discussion.....	25
3.3.	Conclusion	26
Chapter 4.	Software design.....	27
4.1.	Electrodes configuration and motion design.....	27
4.2.	System period characteristic analysis	29
4.3.	Motion classification.....	31

4.3.1	Auto threshold value adjustment	33
4.3.2	Overshoot detection	36
4.3.3	No movement protection.....	37
4.4.	System simulation.....	38
4.5.	Evaluation of wheelchair control	40
4.6.	Conclusion	40
Chapter 5.	Summary	42
5.1.	Conclusion	42
5.2.	Recommendations for future work	43

APPENDIX

Appendix I	Published papers.....	49
Paper 1	Development of a bioimpedance-based human machine interface for wheelchair control	50
Paper 2	A Novel Design and Development on Bioimpedance-Based Wheelchair Control	54
Paper 3	Evaluation of human machine interface for wheelchair control with bioimpedance.....	58
Appendix II	Simulation results of volunteers.....	60
Appendix II.1	Mr. Huang Yunfei's test result	61
Appendix II.2	Mr. Wang Shenming's test result	62
Appendix II.3	Mr. Xu shubing's test result	62
Appendix II.4	Mr. Wang Xianwei's test result.....	64
Appendix II.5	Mr. Wang Xianwei's test result.....	65
Appendix III	HIOKI 3531 Z HITESTER.....	66
Vitae	75

LIST OF TABLES

Table 1	Wheelchair motion design.....	28
Table 2	The motion description of the interface	28
Table 3	Evaluation subject detail description.....	40

LIST OF FIGURES IN TEXT

Figure 1-1	Methodology.....	5
Figure 2-1	Human machine interface (HMI)	7
Figure 2-2	Structure of human device interface in modeling stage	8
Figure 2-3	Structure of human device interface in practical stage.....	8
Figure 2-4	2R-1C serial circuit and frequency response.....	11
Figure 2-5	Four-electrode method.....	14
Figure 3-1	Block diagram of the bioimpedance measurement.....	15
Figure 3-2	Modified Howland voltage controlled current source.....	16
Figure 3-3	Impedance of resistor at different frequency tested by HIOKI 3531 Z HITESTER.....	17
Figure 3-4	Current source frequency response curve(R-I-F)	19
Figure 3-5	1.2 k Ω resistor impedance at different frequency	20
Figure 3-6	Right shoulder impedance (magnitude) at different frequency.....	21
Figure 3-7	Right shoulder impedance change at different frequency	22
Figure 3-8	The 3M™ 2223 Monitoring Electrodes	23
Figure 3-9	NI PCI 6250 DAQ device.....	24
Figure 3-10	CB-68LP(left) and PCI 6250 DAQ device(right) pinout.....	24
Figure 3-11	NI PCI 6250 differential input connections for non-referenced signals ..	25
Figure 3-12	Tested impedance larger than the normal one.....	26
Figure 4-1	Electrodes configuration.....	27
Figure 4-2	Movement period analysis.....	29
Figure 4-3	Flow chart of motion detection algorithm	32
Figure 4-4	Illustration of the threshold value adjustment	35
Figure 4-5	Bioimpedance signal classification result.....	36
Figure 4-6	LED control simulation panel.....	39
Figure 4-7	Wheelchair control simulation panel.....	39

LIST OF FIGURES IN APPENDIX

Figure A 1	Mr. Huang Yunfei and his five simulation tracks.....	61
Figure A 2	Mr. Wang Shenming and his five simulation tracks.....	62
Figure A 3	Mr. Xu Shubing and his five simulation tracks	63
Figure A 4	Mr. Wang Xianwei and his five simulation tracks.....	64
Figure A 5	Mr. Fu Dongjin and his five simulation tracks	65

Chapter 1. Introduction

1.1. Importance of research and problem statement

Statistical data shows that the war and accident not only cause a lot of deaths but also made more than 10 millions of the handicapped. In addition, disease is another reason that caused the handicapped. The number is still increasing second by second. There are so many of the handicapped who suffer from the inconvenience for their daily life, especially for those deep disabled ones. Examples are the populations who have the spinal cord injury (SCI), myelopathy, upper limb disabled, lower arm disabled, loss of skeletal muscle control from below the shoulders and hand amputees. The limitations imposed by these diseases deprive the injured individuals from operating electronic devices like computers or mobile devices. Besides they have poor quality of lives because of the impairments. They also face a communication problem because they are not able to operate devices that make possible to communicate with others such as computer, cell phone, and PDA. Researchers from all over the world concern to help them to improve their life quality by rebuilding the capability for communication and control [1]. So, there is a large amount of requirement for the assistant devices for those populations.

A number of related works in grasping, virtual reality and gesture-based user interfaces have shown the potential application for the handicapped control [2]. Researchers not only use eye-movement, brain function, residual muscle capacities, sip-puff switches or other less traditional devices like mouth-sticks, chin and hand switches, vocal joysticks, and breath mouse but also try to utilize the myoelectric signal EMG, EOG and EEG as a control source for those application. Even many assistive technologies have been developed to help some of the individuals' limitation, there are still large gaps that need to be bridged in order to improve disabled users' ability to interact with personal computers and the surrounding environment.

Prosthesis and wheelchair are the main research area of myoelectric control systems. Prosthesis is the most important and potential application. The ‘‘Utah arm-elbow’’, ‘‘LTI boston arm’’, and ‘‘Otto bock arm-elbow’’, are currently available myoelectric prostheses. They are based on microprocessor and can be programmed for different motions depending on the researcher [2]. Wheelchair control is another important application of myoelectric control systems. In the real world today, the use of wheelchairs has increased rapidly. That is due to the fact that the elders need to use the wheelchair as well as the disabled people. As everybody knows, wheelchairs undoubtedly play an important role in helping those populations who damaged their bodies or legs severely to engage in social activities freely [7]. There are many researchers working on the EMG based electric wheelchair [7][8][9][10]. Their designs consist of at least 4 motions, i.e. stop, forward, turn left and turn right.

In this study, we developed a bioimpedance based human machine interface for the handicapped and the elderly who cannot use their hands and arm to control the wheelchair. Only three electrodes were used in our system. Operations for users are achieved to control the wheelchair smoothly and easily. The performance of the proposed system was evaluated on a map in the LabVIEW 8.2 software environment.

1.2. Literature review

There are four strong points of bioimpedance. Firstly, the current source frequency for bioimpedance signal detection is given by the researcher while the other method has a very narrow bandwidth. Frequency from 0.2 to 3.0Hz is responsive to bio-potentials generated by eye motions (EOG). The frequency range related to EEG signal is from 0.5 to 45Hz and EMG is detected between 70-1000 Hz [10]. So we can apply a frequency range from 20k to 100 kHz in case to interfere the other bio-medical signal. Secondly, the amplitude of bioimpedance signal is much larger than the EMG. That makes the measurement much easier. The EMG signal amplitude by voluntary contraction is measured in 0 to 10 mVp.p range [13]. When we injected a constant current, the bioimpedance change between the measuring electrodes is directly

proportional to the intensity of segment movement. This voltage is relatively low. When a 1-mA current was excited, the relatively voltages vary between 20 and 70mV [14] for the typical magnitudes of the measured impedances which in the range of 20-70 Ω . Thirdly, impedance signals characteristic is the same on a given segment for healthy subjects at rest time and special invariant, even it is in different time and different space [15]. Fourthly, because it is non-injective method, we can examine the subject without any pain or wounds. Furthermore, the system for bioimpedance measure is cheap and easy to handle. [16].

However, weak points of the bioimpedance signal also exist. The bioimpedance signal in limbs (chest, pelvis, thigh, calf) is influenced by the heartbeat, which caused by the cardiac output. But they have the same pattern [15]. For different segment and different individual, the absolute impedance values are different. In addition, it is not possible to recognize the multi-joint movement directly beyond of signal processing [3]. But it is not a large problem because the magnitude of the heartbeat effect is not high. We can avoid that by adjusting the threshold value. For the multi-joint movement detection, we can handle it by increasing measurement channels and use some advanced algorithm.

Although some conventional methods such as electro-goniometer, electromyography, and video camera exist, bioimpedance is still suitable for analyzing the movement of human tissue compared to other signals. Each type of technique has its advantages and disadvantages. Goniometry is a good equipment to analyze human movement in one degree of freedom. However, in the multiple degrees of freedom, it is not a good option for detecting fast or complex movements. Electromyography is difficult to determine kinetic parameters as EMG signals are not linear proportional to the associated movement. In the way of camera and video analyzing, the picture from a camera cannot be processed quickly because it takes a lot of time to do the image processing while video analyzer is very expensive and complex [3]. On the other hand, the method of bioimpedance is simple, less expensive and requires very little space. The most important point is that bioimpedance conveys kinematic information which makes the amplitude change of the signal proportional to the movement of segment. Moreover, this signal change can be kept. We can make a full use on this point.

People study bioimpedance to analyze the composition of human body which can diagnose some kinds of disease and to analyze the movement of the human body which can help to develop the prosthesis and friendly human machine interface. Composition analysis is the main study field. However, in the past few years, some of the researchers already started to study the use of bioimpedance on movement analysis [3][4][5][6]. More and more experts and researchers devote their work in this special field.

1.3. Thesis objective

1. To study the knowledge of bioimpedance signal.
2. To study the optimal setup for bioimpedance signal measurement such as the frequency of current source and electrode configuration.
3. To study the analytical techniques for employing bioimpedance signals as a controlling commands of human machine interface.

1.4. Thesis scope

This research describes the technology of bioimpedance measurement, signal processing and data classification. Human machine interface is also introduced. The study scope is as follows.

1. 5 healthy subjects

Repeat the measurement on the same subject 5 times and compare the results of at the same subject.

2. Age range from 20 to 30
3. Sit on the chair
4. Test frequency in the current source is range from 1 kHz to 200 kHz
5. Implement on LabVIEW 8.2.

1.5. Methodology

Bioimpedance signal processing procedure is shown in Figure 1-1.

1. Data acquisition

The first step of this phase is to configure the electrodes, which use the four electrode method to measure the signal. In order to make the signal processing more convenient, we adopt NI PCI 6250 DAQ board to sample the data and use LabVIEW 8.2 software to save the data in files.

2. Data pre-processing

After measuring bioimpedance signals on the proper locations (muscles), we should analyze the frequency components of the bioimpedance signal by some spectral methods in order to design a suitable filter to reduce most of the noise. Then, according to the result of spectral analysis, we can design the filter easily. Following the noise reduction, it is the signal smoothing.

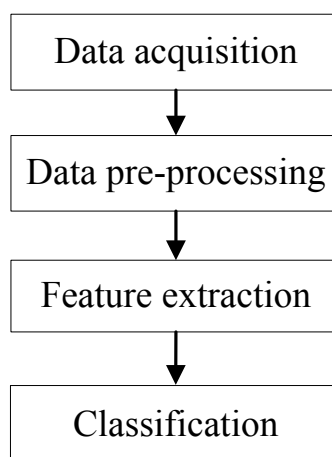


Figure 1-1 Methodology

3. Feature extraction

This module computes and presents preselected features for a classifier. Features, instead of raw signals, are fed into a classifier to improve classification

efficiency. Selection or extraction of highly effective features is one of the most critical stages in myoelectric control design. The time domain feature in this project is based on the magnitude of the bioimpedance. Mean absolute value (MAV) and root mean square value (RMS) are two well-known time domain features. In our thesis we chose RMS and the time that the user holds the action.

4. Classification

A classification module recognizes signal pattern, and classifies them into pre-defined category. To the complexity of biological signals, and the influence of physiological and physical conditions, the classifier should be adequately robust and intelligent. It should be able to adapt itself to changes during long-term operation by exploiting offline and/or online training. Normally, classification depends on the characteristic of the signal.

1.6. Conclusion

In this chapter, it introduces the information about the thesis proposal. It shows the importance of research and problem statement. Second section shows the reason that we choose bioimpedance as a control source. Third section provides objectives in this thesis. Fourth section is the research scope. Fifth section is the methodology used in this thesis.

Chapter 2. Theory

2.1. Human machine interface

Human machine interface (HMI) is one kind of myoelectric control system which is used to interact between mankind and machines, such as computer, robotic arm, prosthesis and wheelchair. The interaction methods can include touch, sight, sound, heat transference or any other physical or cognitive function, which were designed according to the condition of the user. We can see the interfaces function as shown in Figure 2-1. All of the traditional devices only can be used by the normal people, but with the help of the human machine interface, obviously, the disabled populations resume their abilities to communicate and improve their life qualities in a certain extent.

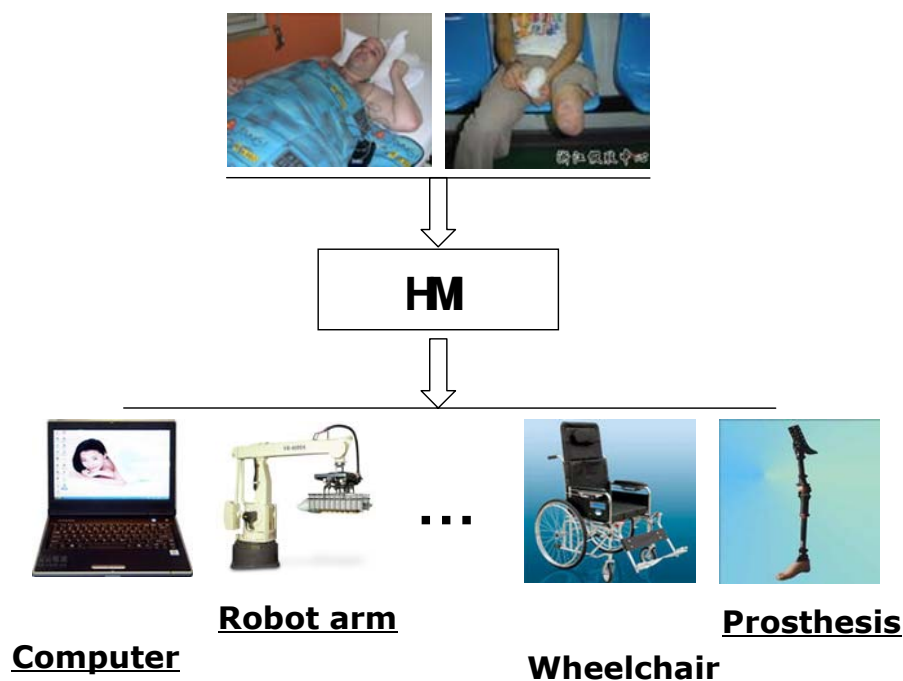


Figure 2-1 Human machine interface (HMI)

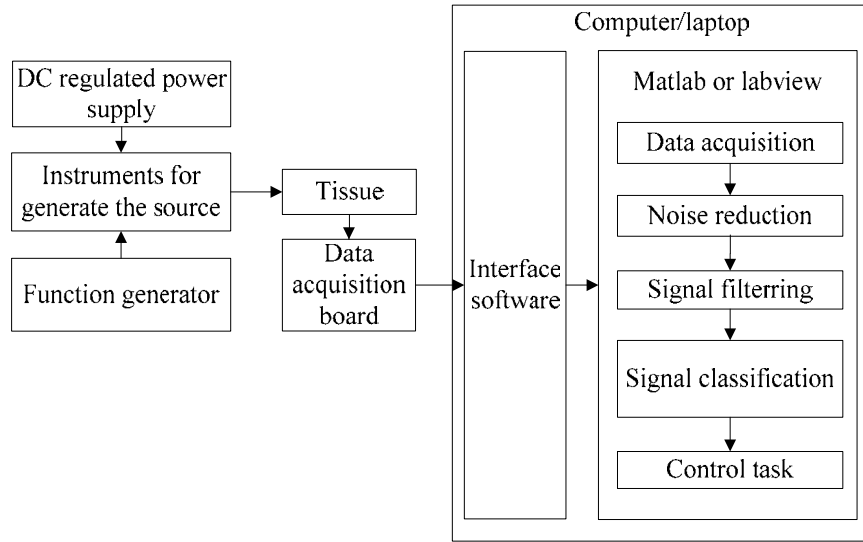


Figure 2-2 Structure of human device interface in modeling stage

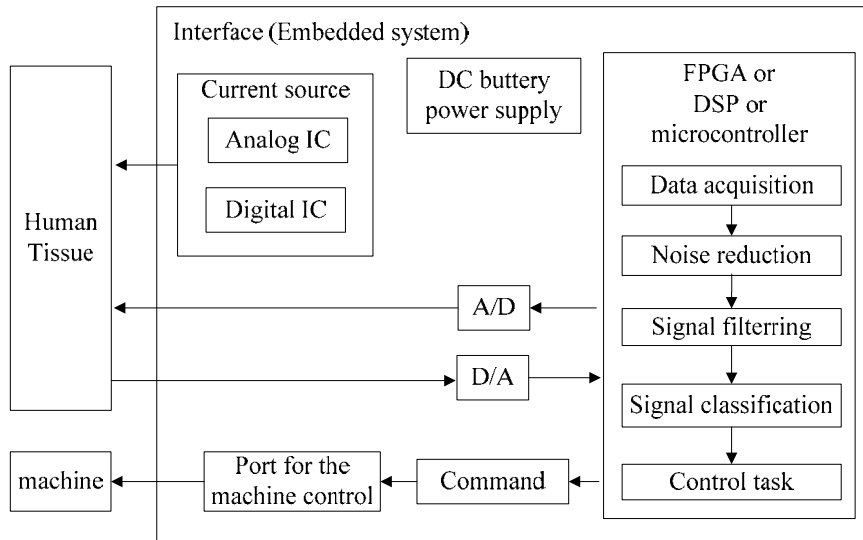


Figure 2-3 Structure of human device interface in practical stage

At the system modeling stage, the excited signal can be generated by a series of instruments. Then, we can use a data acquisition board to collect the signal, and let the computer finish the following work: signal processing, signal classification and system simulation. On the computer, the well-known software for these processes are MATLAB and LabVIEW. MATLAB has its strength in data processing ability while LabVIEW is easy to use due to the abundance of full-function modules. Figure 2-2 shows the flow chart of human-machine interface in modeling stage. But, at the practical stage, normally, the HMI should be portable so that the user can take it easily. It is an embedded control system as shown in Figure 2-3. Everything will be integrated on a single board. DC power supply will be replaced by a battery. Laboratorial equipments will be replaced by the specific IC, and microcontroller will take place of computer to complete data acquisition, signal processing, signal classification and task controlling. The interface only offers data input ports for data acquisition and classified command output to fulfill the control task. As a result, users can take it as easily as take a mobile phone.

2.2. Bioimpedance signals

In biomedical engineering, bioimpedance is a term used to describe the response of a living organism to an externally applied electric current. It has been proved that the bioimpedance measurement of humans and animals is useful for measuring such things as blood flow and body composition [11].

In bioimpedance plethysmography, the measure is sometimes based on pulsatile blood volume changes in the aorta. Bioimpedance is relevant to the development of devices to measure cardiac output and circulating blood volume. Electrical conductivity can vary as a result of breathing. Because of this and other sources of variability, the reliability of bioimpedance for obtaining accurate data has been called into question. Nevertheless, the technique is used in both routine clinical medicine and research [11].

Biological materials such as blood and muscle are poor conductors, relative to materials classified as conductors, (e.g., copper) at frequencies most often

used for measuring physiological activity ($f < 10^6$ Hz). At higher frequencies, these biological materials have resistive and dielectric properties, and at even higher frequencies, behave as dielectrics. The frequencies of interest for assessing physiological activity by impedance are usually in the range of 20 kHz to 100 kHz. In order to get rid of the influence of phenomenon such as ECG, EEG, and EMG, the lower limit frequency is selected at 20 kHz. In the meanwhile, the current intensities should not be higher than a few milli amperes to avoid stimulating muscles and nerves [12].

2.3. Bioimpedance equivalent circuit

Human tissue has both resistive and capacitive properties. There are many equivalent circuits has been brought forward to describe the electrical characteristic. Normally, the most used one consists of three components. It may comprise two resistors and one capacitor or two capacitors and one resistor. Figure 2-4 shows bioimpedance serial equivalent circuit with two resistors and one capacitor. The circuit allows DC current, and guarantees current limitation at high frequencies. It is possible to obtain the same immittance values for all frequencies with only one set of component values. The series version is best characterized by impedance because the time constant then is uniquely defined (in equation 2.1-2.7). It has often been used as a skin electrical equivalent, with R for deeper tissue in series and the skin composed of G and C in parallel. In addition, the frequency response of this circuit is also plotted in Figure 2-4. The serial 2R-1C model can be described by the following equations:

$$Z = R + \frac{G - j\omega C}{G^2 + \omega^2 C^2} \quad (2.1)$$

$$Z = R + \frac{1}{G(1 + j\omega\tau_z)}$$

$$\tau_z = \frac{C}{G} \quad (2.2)$$

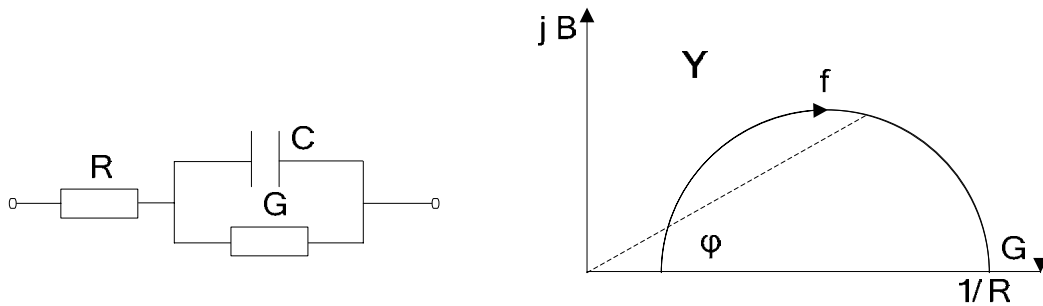


Figure 2-4 2R-1C serial circuit and frequency response

$$\varphi = \arctan\left(\frac{\omega C}{G(1+RG) + \omega^2 C^2 R}\right) \quad (2.3)$$

$$\varphi = \arctan\left(\frac{\omega C}{G(1+RG + \omega^2 \tau_z \tau_2)}\right)$$

$$Y = \frac{G(1+RG) + \omega^2 C^2 R + j\omega C}{(1+RG)^2 + \omega^2 C^2 R^2} \quad (2.4)$$

$$Y = \frac{G(1+RG + \omega^2 \tau_z \tau_2 + j\omega \tau_z)}{(1+RG)^2 + (\omega \tau_2)^2}$$

$$\tau_2 = CR \quad (2.5)$$

$$C_{\text{ext}} = \varepsilon' = \frac{C}{(1+RG)^2 + (\omega \tau_2)^2} \quad (2.6)$$

$$\varepsilon'' = \frac{G(1+RG + \omega^2 \tau_z \tau_2)}{\omega[(1+RG)^2 + (\omega \tau_2)^2]} \quad (2.7)$$

Impedance is the preferred parameter characterizing the two resistors, one capacitor series circuit, because it is defined by one unique time constant τ_z (eq. 2.2). This time constant is independent of R, as if the circuit was current driven. The impedance parameter therefore has the advantage that measured characteristic frequency determining τ_z is directly related to the capacitance and parallel conductance (e.g. membrane effects in tissue), undisturbed by an access resistance. The same is not true for the admittance: the admittance is dependent both on τ_z and τ_2 , and therefore on both R and G.

when $\omega \longrightarrow 0$

$$\begin{aligned}
 Y &\longrightarrow G/(1+RG) \\
 B &\longrightarrow \omega C/(1+RG)^2 \\
 C_{ext} &\longrightarrow C/(1+RG)^2 \\
 \varphi &\longrightarrow 0^\circ
 \end{aligned} \tag{2.8}$$

when $\omega \longrightarrow \infty$

$$\begin{aligned}
 Y &\longrightarrow 1/R \\
 B &\longrightarrow \omega C / \omega^2 C^2 R^2 \longrightarrow 0 \\
 C_{ext} &\longrightarrow C / \omega^2 C^2 R^2 \longrightarrow 0 \\
 \varphi &\longrightarrow 0^\circ
 \end{aligned} \tag{2.9}$$

Equation (2.9) is of particular interest. C_{ext} is the capacitance measured on the terminals, for example, with a bridge or a lock-in amplifier. At high frequencies the susceptance part $B = Y''$ is small, and C_{ext} is strongly frequency dependent ($1/\omega^2$). In this frequency range, the strong capacitance increases with decreasing frequency. It is externally true as measured at the network port. But it does not reflect any frequency dependence of the internal capacitor component. It only reflects the simple fact that we do not have direct access to the capacitor, only through the (at high frequencies) dominating series resistance R .

2.4. The effective factor of bioimpedance

Human tissue also can be seen as the parallel conductor model which consists of muscle and blood. Bioimpedance is expressed by

$$Z = \frac{L}{\sigma_m S_m + \sigma_b S_b} = \frac{L}{\sigma_m S_m + \sigma_b V_b / L}, \tag{2.10}$$

Where σ_m = conductivity of muscle; σ_b = conductivity of blood; S_m = sectional area of muscular tissue; S_b = sectional area of blood vessel; L = length of measured part; and V_b = volume of blood. If we keep on monitoring the change of impedance, L is a constant. Because after put the electrodes on the tissue, we do not move it anymore. During we make a movement, the change of σ_m and σ_b are very small, so that they do not have to be taken into account. Meanwhile, the sectional area of blood vessel is pretty small, it does not effect on the impedance change too much. Finally, the change of impedance is mainly caused by V_b and S_m [17].

2.5. Four electrodes method

In order to reduce the zones to the stimulated electrodes and the polarization impedance of the electrodes themselves, four electrodes method is considered.

Normally, the researchers [3][4][5][6][14][15][16][17][19] adopted the four electrodes method as the measurement system. The system was shown in Figure 2-5. As we can see, one pair of electrodes excite the ac constant current to the tissue of human body, another pair of electrodes detect the potential difference between themselves. We can find the bioimpedance Z by Ohm's law

$$Z = \frac{V}{I}, \quad (2.11)$$

where V is the voltage and I is the current.

In our project, it is not necessary to calculate the exactly impedance, because the tested voltage reflect the impedance change which we are interested in. It is also can be express by Ohm's law

$$V = I \times Z, \quad (2.12)$$

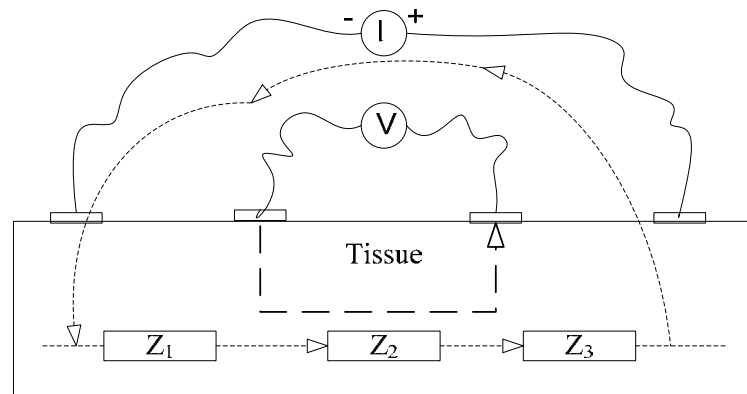


Figure 2-5 Four-electrode method

2.6. Conclusion

This chapter is about the theory. It describes the basic knowledge related in this thesis work. In section one, it provides the definition, the function and the common structure of the human device interface (HDI). Section two explains the conception and the characteristic of the bioimpedance, researchers' objectives using bioimpedance. In section three, it shows the equivalent circuit of human tissue to provide the impedance property of human tissue. Section four, it used an equation demonstrated the factors that effect to the change of bioimpedance, as it help us to find an optimal electrode configuration. In section five, a basic bioimpedance measurement method: four electrodes method is introduced.

Chapter 3. Hardware design

3.1. System configuration

Figure 3-1 shows a block diagram of the bioimpedance measurement system. DC power supply was used to supply the power. A current source was made by a SG-4101 function generator and a modified Howland bridge voltage controlled current source (VCCS). VCCS converts a 50 kHz voltage signal, generated by a function generator, into a 50 kHz 0.3 mA sinusoidal ac current. Current was excited at the shoulders of the user. Two channels of NI PCI-6250 DAQ board were used to acquire the data at sampling frequency of 600 kHz for each channel. After data acquisition, the signal storing, processing, classification and system simulation would all be done on the computer by LabVIEW 8.2 software.

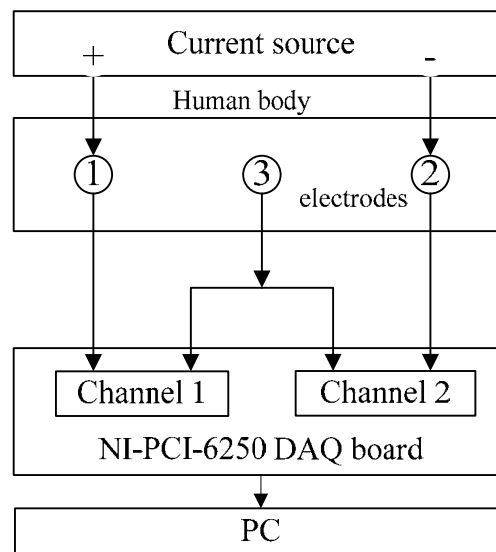


Figure 3-1 Block diagram of the bioimpedance measurement

3.1.1 Current source

3.1.1.1 Current source design

In the current source design, the basic requirements are: high output impedance and wide frequency band. The modified Howland VCCS shown in Figure 3-2 is fulfilled these conditions. It is made of two high frequency, low noise operational amplifiers (LF 412CN) and five metal film resistors. It transforms the sine wave voltage signal to the constant sine wave current signal. When the circuit meets the condition

$$\frac{R_2}{R_1} = \frac{R_4}{R_3}, \quad (3.1)$$

the output impedance $R_o = \infty$. And load current can be calculated as the following equation

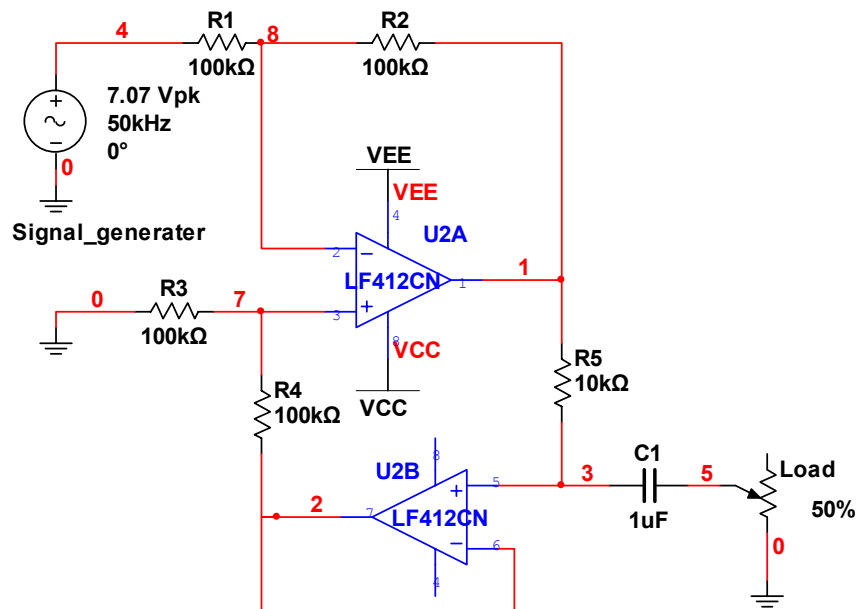


Figure 3-2 Modified Howland voltage controlled current source

$$I = V_1 / R_5, \quad (3.2)$$

where V_1 is root mean square value of input voltage signal generated by SG-4101 function generator.

3.1.1.2 General resistor property analysis

After put the design into practice, it is a necessary to calibrate the current source, see if it is up to the mustard. In order to fulfill this mission, we should find a standard resistor, for setting the current beforehand. So, we tested the resistor (10 Ω , 120 Ω , 300 Ω , 510 Ω , 1000 Ω) on HIOKI 3531 Z HITESTER (appendix III), and recorded their impedance at different frequency. Figure 3-3 shows the result of the test, resistor's impedance changes almost focus at two segment of frequency range: from 10 kHz to 30 kHz, and from 90 kHz to 100 kHz. They are almost constant in range from 30 kHz to 90 kHz. And another important characteristic is the larger the resistor, the smaller the change of impedance. As we can see, 1 k Ω resistor change very little when the frequency change. So it will be a good choice to use a resistor larger than 1 k Ω as a standard resistor for the current source test.

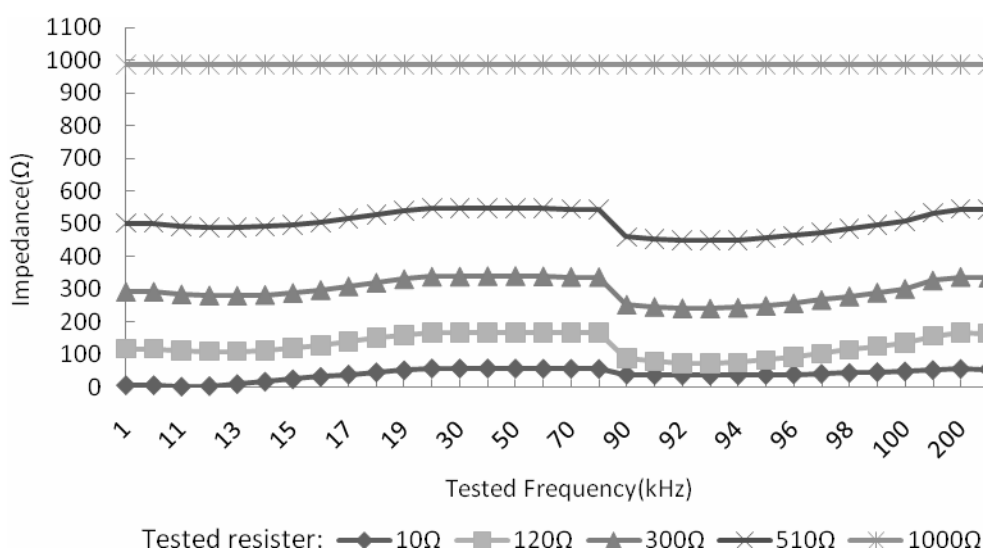


Figure 3-3 Impedance of resistor at different frequency tested by HIOKI 3531 Z HITESTER

3.1.1.3 Current source performance analysis

After simulation on the software Multisim10.0, a PCB board was made to test the performance of the current source. As the objective is to measure the electrical impedance of human tissue and find out an optimal frequency for the movement detection. Even the frequency will be changed during previous experiments for search the optimal frequency, but actually, in the final interface the frequency will not be changed. The only factor that will change is the electrical impedance. So, we tested the response of the current source when the load changes. The scenario for test the load response is designed as:

- 1) Test the response of the resistor (10 Ω , 51 Ω , 120 Ω , 300 Ω , 510 Ω , 1000 Ω) at different frequency range from 10 kHz to 250 kHz by HIOKI 3531 Z HITESTER, in order to find the standard resistor for setting the current source.
- 2) Set the function generator to sine wave channel;
- 3) Setting a certain frequency (10 kHz);
- 4) Adjust the voltage signal generator to set the current source to be 500 μA at a specified resistor which has a 1000 Ω impedance;
- 5) Using oscilloscope to measure the root mean square (RMS) voltage value of the load which are 100 Ω , 500 Ω , 800 Ω , 1 k Ω , 2 k Ω , 3 k Ω and 4 k Ω respectively, as human body tissue is not high. And then plot in the figure, we can get the load response curve of the current source.
- 6) Setting the frequency to be 20 kHz, 40 kHz, 50 kHz, 75 kHz, 100 kHz, 125 kHz, 150 kHz, 175 kHz and 200 kHz respectively to get the load response of the current source.

In the end, we can get the performance of current source at different load and different frequency from Figure 3-4. As we can see from all of the curves, even at the high frequency of 200 kHz and high load value of 1 k Ω . The error of current source is less than 2%. This precision of the current already meets our requirement.

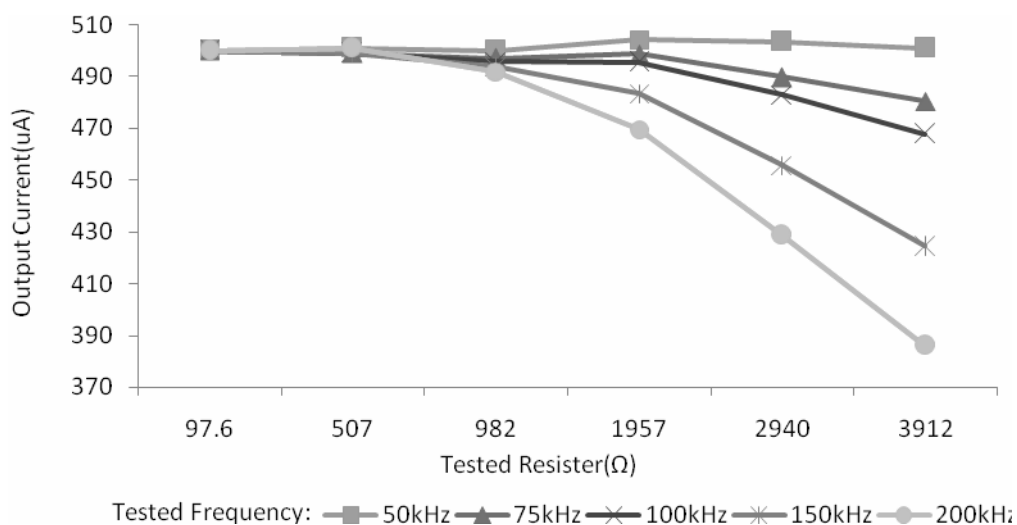


Figure 3-4 Current source frequency response curve(R-I-F)

Anyway, NI PCI 6250 device also is used to collect the root mean square value of a 1.2 k Ω resistor at different frequency to demonstrate that the current source is reliable. This scenario is:

- 1) Chose a 1.2 k Ω resistor as a standard resistor;
- 2) Set the function generator to sine wave channel;
- 3) Set a certain frequency 50 kHz;
- 4) Set current magnitude to 0.3 mA;
- 5) Record all the root mean square value of 1.2 k Ω resistor at the frequency range from 1 kHz to 200 kHz;
- 6) Plot out the curve and find the characteristic.

The fact is that the current source is very stable at the frequency range (10k~140 kHz), see from Figure 3-5. The frequency band is enough for the experimental request.

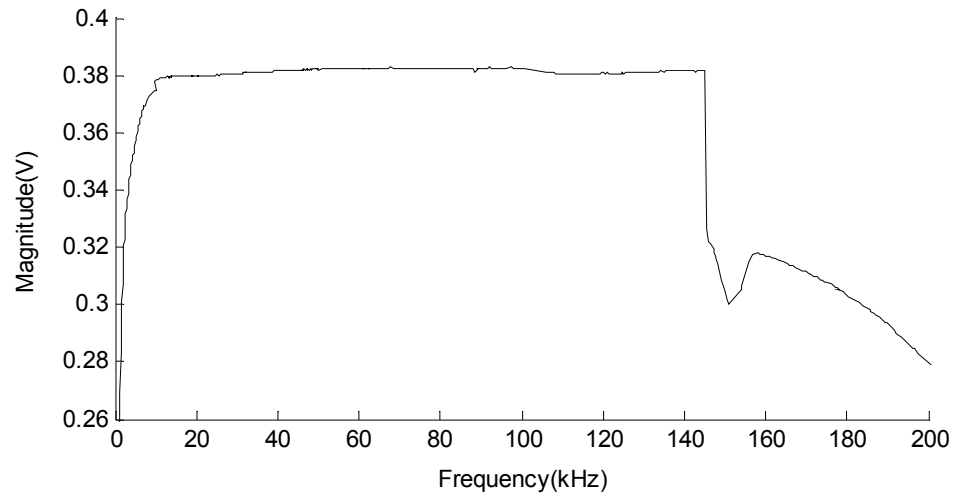


Figure 3-5 1.2 k Ω resistor impedance at different frequency

3.1.2 Current source frequency selection

The frequency selection for bioimpedance measurement was proposed since from the beginning of this study. In order to find the optimal frequency for movement detection, scenarios are designed as following:

Scenario one, finding out the relationship between tissue voltage magnitude and current source frequency:

- 1) Stick electrodes on the shoulders (follow the electrodes configuration);
- 2) Set the function generator to sine wave channel;
- 3) Set the current source as 0.3 mA at 50 kHz;
- 4) Connect the system correctly and run LabVIEW 8.2 to Collect the root mean square value of right shoulder;
- 5) Change the frequency from 1 kHz till 200 kHz step by 1 kHz;
- 6) Stop LabVIEW 8.2 program;
- 7) Plot the root mean square value graph of right shoulder.

Figure 3-6 shows the result of Right shoulder impedance (magnitude) at different frequency. It illustrate that the impedance magnitude is inverse ratio to the frequency.

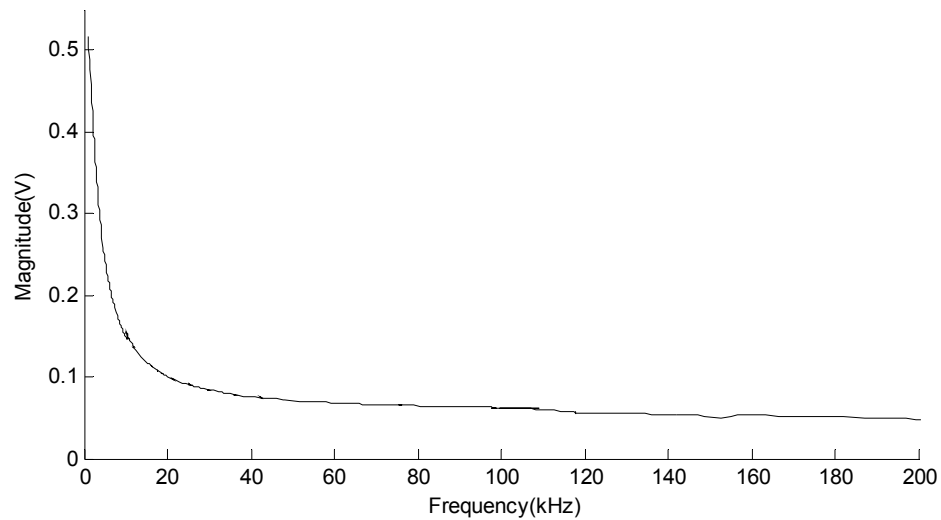


Figure 3-6 Right shoulder impedance (magnitude) at different frequency

Scenario two, finding out the relationship between right shoulder impedance change and frequency:

- 1) Stick electrodes on the shoulders (follow the electrodes configuration);
- 2) Set the function generator to sine wave channel;
- 3) Set the current source as 0.3mA at 50 kHz;
- 4) Connect the system correctly and run LabVIEW 8.2, Read the maximal root mean square value change (impedance change) of right shoulder and write it into excel file;
- 5) Change the frequency from 1 kHz to 200 kHz by 5 kHz per step and move shoulder up and down at each step and record the maximal change into excel file according to the frequency;
- 6) Stop LabVIEW 8.2 program;
- 7) Plot the root mean square value graph of right shoulder (data from the excel file).

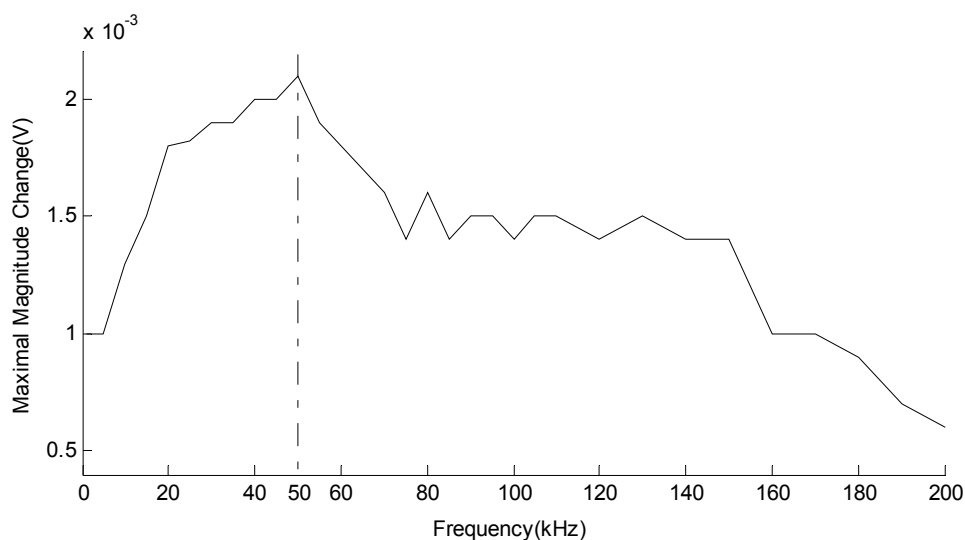


Figure 3-7 Right shoulder impedance change at different frequency

Figure 3-7 is a graph of the right shoulder impedance change to the different frequency. The maximal change was 2.1 mV found at 50 kHz, by the left side of this point, the change increasing with frequency increasing, while by the right side, it is decreasing with the frequency increasing. It is demonstrated that 50 kHz current source is the optimal choice for the movement monitoring. This result is applied in our study.

3.1.3 Monitoring electrodes

The 3M™ 2223 Monitoring Electrode in Figure 3-8, fulfills the AAMI EC-12 (2000) standard, is small Monitoring Electrode for short term applications. It has the following physical features: size is diameter 3 cm, thickness is 0.8 cm, backing is foam, adhesive is hypoallergenic and acrylic adhesive, and conductor is dry gel and hydrophilic synthetic polymer. It is class I medical device which is easy to handle and apply, conformable, high patient comfort, used both in adult and paediatric, fluid resistant, added tab for easy removal, quick and reliable trace and latex free. It is primary used in operating room and emergency room. It will be a good choice to use disposable sensors in our application.



Figure 3-8 The 3M™ 2223 Monitoring Electrodes

3.1.4 NI PCI 6250 DAQ device

NI PCI 6250 board is a 16-Bit, 1 MS/s (multi-channel), 1.25 MS/s (single channel), 16 analog inputs, 24 digital I/O, high speed M serials data acquisition device. Figure 3-9 shows NI PCI 6250 device (3) and its related hardware: (1) CB-68LP, 68-Pin Digital and Trigger I/O Terminal Block; (2) 68 pin PCI cable; (4) LG personal computer. After connecting the signal channels to (1), (1) connecting to (2), (2) connecting to (3) and (3) connecting to (4) correctly, respectively. We can start to sample data if LabVIEW 8.2, driver and DAQ software were installed properly.

In the NI PCI 6250 board application, at the condition of: (a), The input signal is low-level (less than 1 V); (b), The leads connecting the signal to the DAQ device are longer than 10 ft (3 m); (c), The input signal requires a separate ground-reference point or return signal; (d), The signal leads travel through noisy environments. The connect mode requested to be differential connection. Differential signal connections reduce noise pickup and increase common-mode noise rejection. Differential signal connections also allow input signals to float within the common-mode limits of the instrumentation amplifier. As our application meet condition (a) therefore we have to connect each channel as the differential connection mode.

A differential connection is one in which the DAQ device AI signal has its own reference signal, or signal return path. These connections are available when the selected channel is configured in DIFF input mode. Figure 3-10 shows pinout of

connector CB-68LP and PCI 6250 DAQ device. The differential analog input channel i consists of two single analog input pins $AI\langle i \rangle$ and $AI\langle i+8 \rangle$. $AI\langle i \rangle$ is the positive input while $AI\langle i+8 \rangle$ is the negative input. $AI\langle i \rangle$, $AI\langle i+8 \rangle$ and $AI\text{ GND}$ must be connected properly, if not, it may cause the wrong sampled signal. In addition, if the input is a float source, it is necessary to add a bias resistor between $AI\langle i \rangle$ or $AI\langle i+8 \rangle$ and $AI\text{ GND}$ as shown in Figure 3-11. This resistor provides a return path for the ± 200 pA bias current. A resistor value of $10\text{ k}\Omega$ to $100\text{ k}\Omega$ is usually sufficient. If do not use the resistor, the source is truly floating, the source is not likely to remain within the common-mode signal range of the PGIA (instrument amplifier on PCI 6250 board), and the PGIA saturates, causing erroneous readings. Also, you must reference the source to the respective channel ground.



Figure 3-9 NI PCI 6250 DAQ device

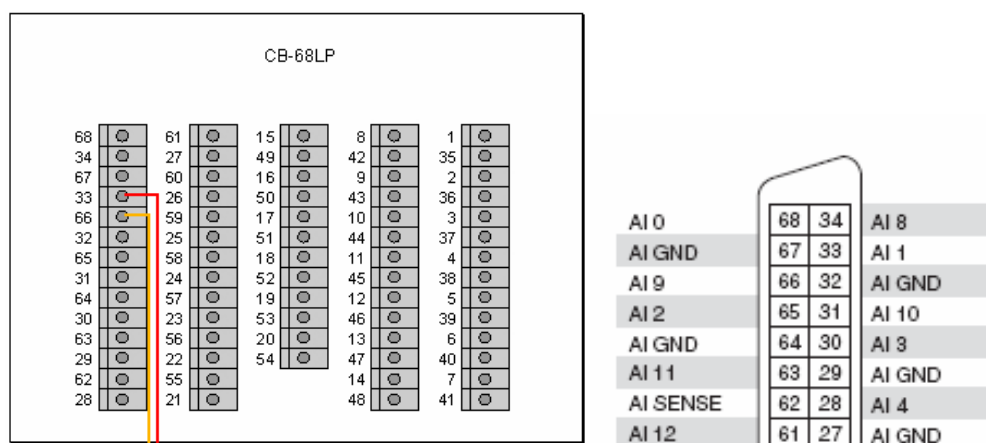


Figure 3-10 CB-68LP(left) and PCI 6250 DAQ device(right) pinout

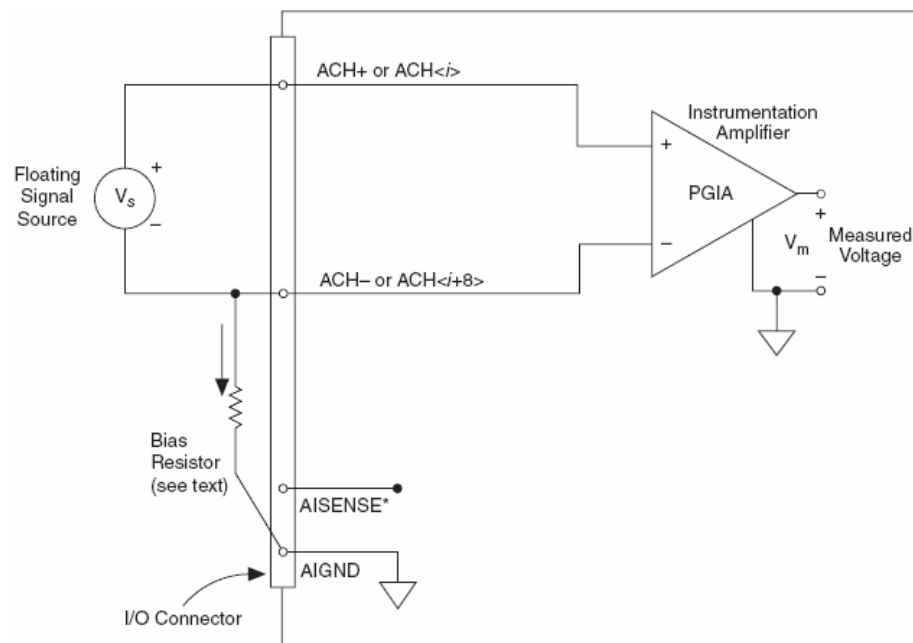


Figure 3-11 NI PCI 6250 differential input connections for non-referenced signals

3.2. Discussion

In the literature review, the value of bioimpedance that researchers present is around 40Ω for 10 cm tissue at forearm. But from our experiment, the result is much higher than in the literatures, i.e., in the range of 200Ω to 500Ω . This may cause by the electrode impedance. Also, the different electrode has different value of impedance. The measured impedance Z_{measured} consists of $Z_{\text{electrode1}}$ = the impedance of electrode 1, $Z_{\text{electrode2}}$ = the impedance of electrode 2, Z_{tissue} = the impedance of human tissue as shown in equation (3.3) also in Figure 3-12.

$$Z_{\text{measured}} = Z_{\text{electrode1}} + Z_{\text{electrode2}} + Z_{\text{tissue}} \quad (3.3)$$

One way of reducing the effect of electrode polarization is to increase the impedance of the sample by increasing its length. However, it is not convenient in our project because the electrodes' configuration is fixed. In order to compensate for the polarization impedance further, several methods are possible:

- 1) Four-electrode system (tetrapolar).
- 2) Measure electrode polarization impedance separately and subtract.
- 3) Substitute the unknown with a known sample for calibration.
- 4) Vary the measured sample length, for example, in suspensions.

Methods 2 and 3 are based on the assumption that the metal–liquid interphase and thus the polarization impedance is invariable. This is not always the case. Measuring on “dry” samples, for instance, implies poor control of the contact electrolyte. Also a sample may contain local regions of reduced conductivity near the electrode surface. The currents are then canalized with uneven current density at the metal surface (shielding effect). Electrode polarization impedance, in particular at low frequencies, is then dependent on the degree of shielding [18].

3.3. Conclusion

Chapter three describes the hardware mentioned in this thesis. It introduces the system configuration of our system, and after that each piece of the system are described in detail.

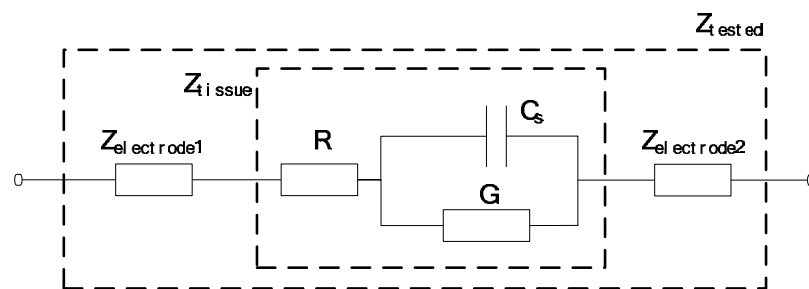


Figure 3-12 Tested impedance larger than the normal one

Chapter 4. Software design

4.1. Electrodes configuration and motion design

As the disabled people who cannot use their hands to operate the wheelchair, such as spinal cord injury, myelopathy, upper limb disabled, lower arm disabled, loss of skeletal muscle control from below the shoulders and hand amputees. We need to design the electrodes location as convenient as possible so that these populations can use. In the end, the locations on the trapezius muscle are chosen.

The measurement method is based on the four-electrode method, but we made some improvement according to the specific application and the specific segment. The conventional four electrodes method needs six electrodes for two channels in our application while we just need three. As shown in Figure 4-1. Electrodes number 1 and 2 are used to supply the current to the tissue and each of them also is one of the voltage detecting electrodes for a certain channel. Electrode number 3 is the common end of the two channels.

Bioimpedance can be nearly considered as the kinematic information, because the bioimpedance change follows the segment movement [17]. This is advantage of bioimpedance compared to SEMG signal. So, we can get more benefit which utilizes bioimpedance as a control source than use SEMG.

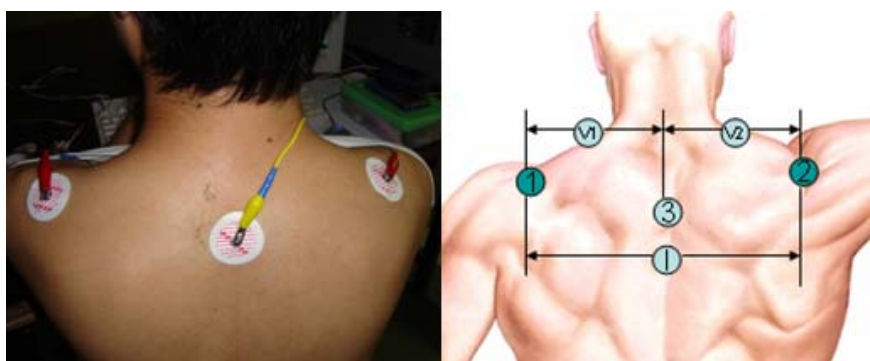


Figure 4-1 Electrodes configuration

Table 1 Wheelchair motion design

Electrode No.	Muscle	Segment	Action hold time	Motion No.
(1,3)	Left trapezius muscle	Left shoulder	300ms<T<1000ms	1
			>1000ms	2
(2,3)	Right trapezius muscle	Right shoulder	300ms<T<1000ms	3
			>1000ms	4
(1,3) (2,3)	Left and right trapezius muscle	Left and right shoulder	300ms<T<1000ms	5
			>1000ms	6

Table 2 The motion description of the interface

Motion NO.	Wheelchair operation	Operation description
1	Turn left 30 degree	If there is a small curve corner, in order to adjust the running direction smoothly during wheelchair running, each command signal makes a 30 degree left side turn.
2	Stop Turn left 90 degree Run	If there is a large angle corner, in order to change the direction rapidly, this command signal will control wheelchair to do serial operation: stop, turn left 90 degree, run
3	Turn right 30 degree	Turn right 30 degree as operation 1
4	Stop Turn right 90 degree Run	Turn right 90 degree as operation 2
5	Stop to run	This operation will be executed when the motion of 6 happen the (2n + 1)th time
	Run to stop	This operation will be executed when the motion of 6 happen the 2nth time
6	Stop Turn 180 degree	This motion will make the “turn back” operation conveniently. Command signal will control wheelchair to do serial operation : stop, turn left 180 degree

Compared to the traditional design of both bioimpedance and SEMG signal application, ours design is more humanistic. In our project, two bioimpedance measure channels were design by three electrodes which can make six kinds of motions which can execute seven serials of operations. The seven serials operations

are: ‘Turn left 30 degree’, ‘Stop; Turn left 90 degree; Run’, ‘Turn right 30 degree’, ‘Stop; Turn right 90 degree; Run’, ‘Stop to run’, ‘Run to stop’, ‘Stop; Turn 180 degree’. The design of motions related to the segment and electrode configuration is shown in Table 1. In addition, Table 2 described the operations related to these motions. It describes the way that the wheelchair operations work and the way that a subject can use this interface to control wheelchair.

4.2. System period characteristic analysis

In order to control the system perfectly, it is necessary to understand all the control situations. There are three situations in a single period of movement as shown in Figure 4-2:

A: there is at least one shoulder up and down movement, but not always hold the shoulder;

B: there is no movement at all;

C: always hold the shoulder in a certain period.

The transfers of these situations will cause different results. In the first case:

$A \rightarrow A$;

$A \rightarrow B$;

$A \rightarrow C$;

The threshold value will be calculated by equation 4.1

$$\text{RMS}_T = (\text{RMS}_{\max} + \text{RMS}_{\min}) / P_S \quad (4.1)$$

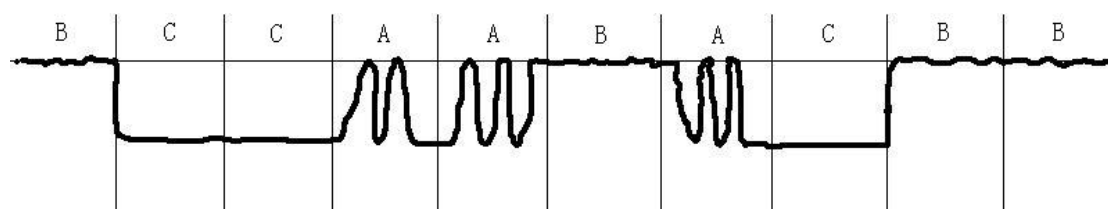


Figure 4-2 Movement period analysis

where RMS_T = natural threshold value, RMS_{max} = maximal root mean square signal value in the array, RMS_{min} = minimal root mean square signal value in the array, P_s = the control sensitivity parameter for the control system. P_s is a very important parameter. It keeps the balance between high control sensitivity and low error rate of operation. This parameter must be modified manually after a subject change or electrodes change (not electrode configuration change). Because the bioimpedance value change is vary from individuals. Even on the same subject, when electrodes were changed, the impedance was different compared with the previous one. In the second case:

B→A;
B→B;
B→C;

The threshold value will be calculated by equation

$$RMS_T = RMS_{min} - P_n, \quad (4.2)$$

where RMS_T is the system threshold value, P_n is a parameter set according to the small change of root mean square value during there is no movement for a long time and RMS_{min} is the same with equation 4.1. While in the third case:

C→A;
C→B;
C→C;

Even the previous period is C, the system will see it as a no movement situation, because when the shoulder was hold and not release, the impedance change just like the change from no movement situation B. As a result, the threshold value will be calculated by equation 4.2. But, indeed, the movement cannot be detected as the threshold value is lower than the minimal signal magnitude. So, we do not suggest to hold a movement for long time duration (>10 second). Even though, this case can be avoid easily, because there is not any necessary and our long time motion is far less than that.

4.3. Motion classification

The control system is implemented on the LabVIEW 8.2 work space. Figure 4-3 shows the flow chart of motion detection algorithm. Details of all steps are as follows.

Step one: 50000 samples of raw bioimpedance signals are collected by NI PCI-6250 DAQ board in real time. There are two reasons for choosing 50000 as the sample number. One is to reduce rate of the random emerge of power line noise. Another is to smooth the signal at the same time with the root mean square value calculation. The more sample was used in root mean square value calculation, the more stable of the signal until 50000. But after 50000, it is almost the same performance to 50000.

Step two: A bandpass filter at the 29 kHz low cutoff frequency and 80 kHz high cutoff frequency will be used to filter the original signal.

Step three: It calculates the root mean square value of the 50000 filtered signals. Equation 4.3 shows the algorithm of the root mean square value calculation,

$$\text{RMS} = \sqrt{\frac{1}{n} \sum_{i=1}^n x_i^2} = \sqrt{\frac{x_1^2 + x_2^2 + \dots + x_n^2}{n}}. \quad (4.3)$$

Step four: Storing the root mean square value (RMS) in an array Arr.

Step five: It checks if it already has collected N (20) samples in array Arr or not. If yes, it will find the maximal root mean square value (RMS_{\max}) and the minimal root mean square value (RMS_{\min}). Then begin to calculate the auto adjust threshold value (RMS_T) for the next period (every N samples is called a period) using equation 4.1. The threshold value used to classify the recent root mean square value is from the previous period. Finally, it will reset the n (the index of array Arr) and go to the next step. If not, program will directly go to the next step.

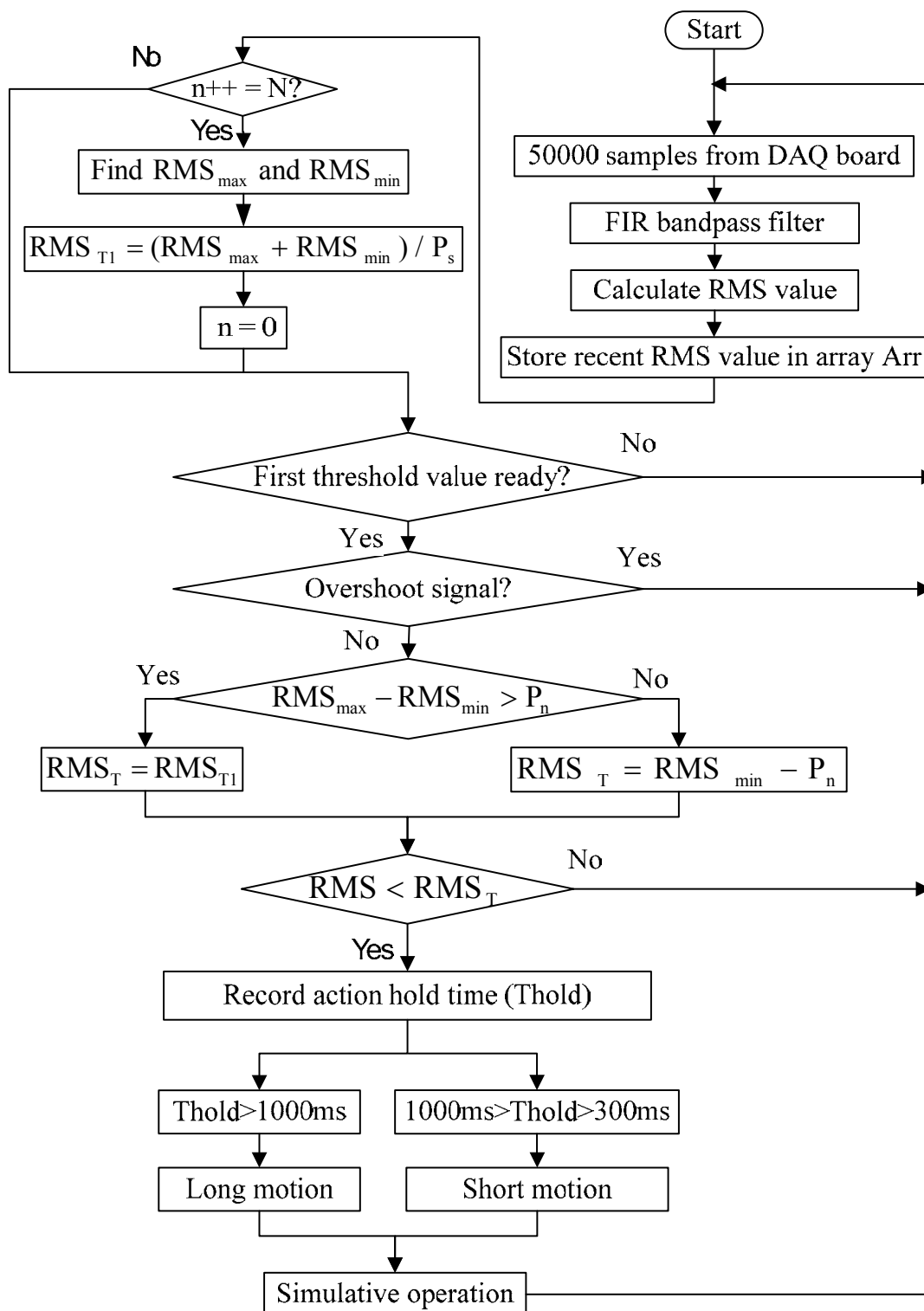


Figure 4-3 Flow chart of motion detection algorithm

Step six: It checks the first threshold value is ready or not. If ready, it starts to classify the recent root mean square value, or it will wait until the generation of the first threshold value.

Step seven: It checks if the recent root mean square value is an unexpected value to avoid the situation that was interfered by some reasons.

Step eight: It judges to use different threshold value, auto adjust threshold value and no-movement-protection threshold value, to classify the recent root mean square value.

Step nine: The action hold time is measured to decide if the motion is a short time motion (action time shorter than 1s but longer than 300ms) or long time motion (action time longer than 1s).

In the end, the classified command will be used to fulfill the control task which is simulation task. There are two simulation phases: in phase one, six motions were used to control the LED on LabVIEW 8.2 panel; while in phase two, they are used to control the wheelchair model run on a map of environment.

4.3.1 Auto threshold value adjustment

The system modifies the nature threshold value every 20 root mean square value. Because the magnitude of the measured signal sometimes changes holistic. If a constant threshold is used, the signal cannot be classified or lead to some wrong classification results. In order to find the new threshold value, system stores 20 root mean square values in an array Arr, find the maximal and minimal value in Arr, and then calculates the threshold value using equation (4.2). Figure 4-4 shows an illustration of the threshold value adjustment. L is left shoulder impedance signal root mean square value and threshold value (the one pix real line is the root mean square value, the two pix dotted line is the no movement protection threshold while the three pix thick real line is the auto adjust threshold value); R is right shoulder impedance signal root mean square value threshold value (the one pix real line is the root mean square value, the two pix dotted line is the no movement protection threshold while the three pix thick real line is the auto adjust threshold value). LS is left shoulder short

time motion; LL is left shoulder long time motion; RS is right shoulder short time motion; RL is right shoulder long time motion; BS is both shoulders short time motion; BL is both shoulders long time motion. Notice that there is a segment of signal is increasing. It is because the current source magnitude was increased in order to show the capability of adjust threshold algorithm. The double rectangles show the works of the no movement protection threshold value. As we can see, the periods before the double rectangle are no movement periods. It demonstrated that the auto adjust threshold value cooperate with no movement protection threshold value work perfectly.

Figure 4-5 shows the root mean square value and classified control command of the filtered bioimpedance signal from both shoulders. It includes all of the movement: left shoulder up and down; right shoulder up and down; both shoulders up and down. In this graph, L is left shoulder impedance signal root mean square value; R is right shoulder impedance signal root mean square value. It is easy to identify the shoulder movement type (short time or long time) from the root mean square value with only our eyes. Obviously, the classified control commands (LS, LL, RS, RL, BS and BL are the same representation with the symbols in Figure 4-4) were following the shoulder movement. And as a result, accuracy of classification is approaching to 100%.

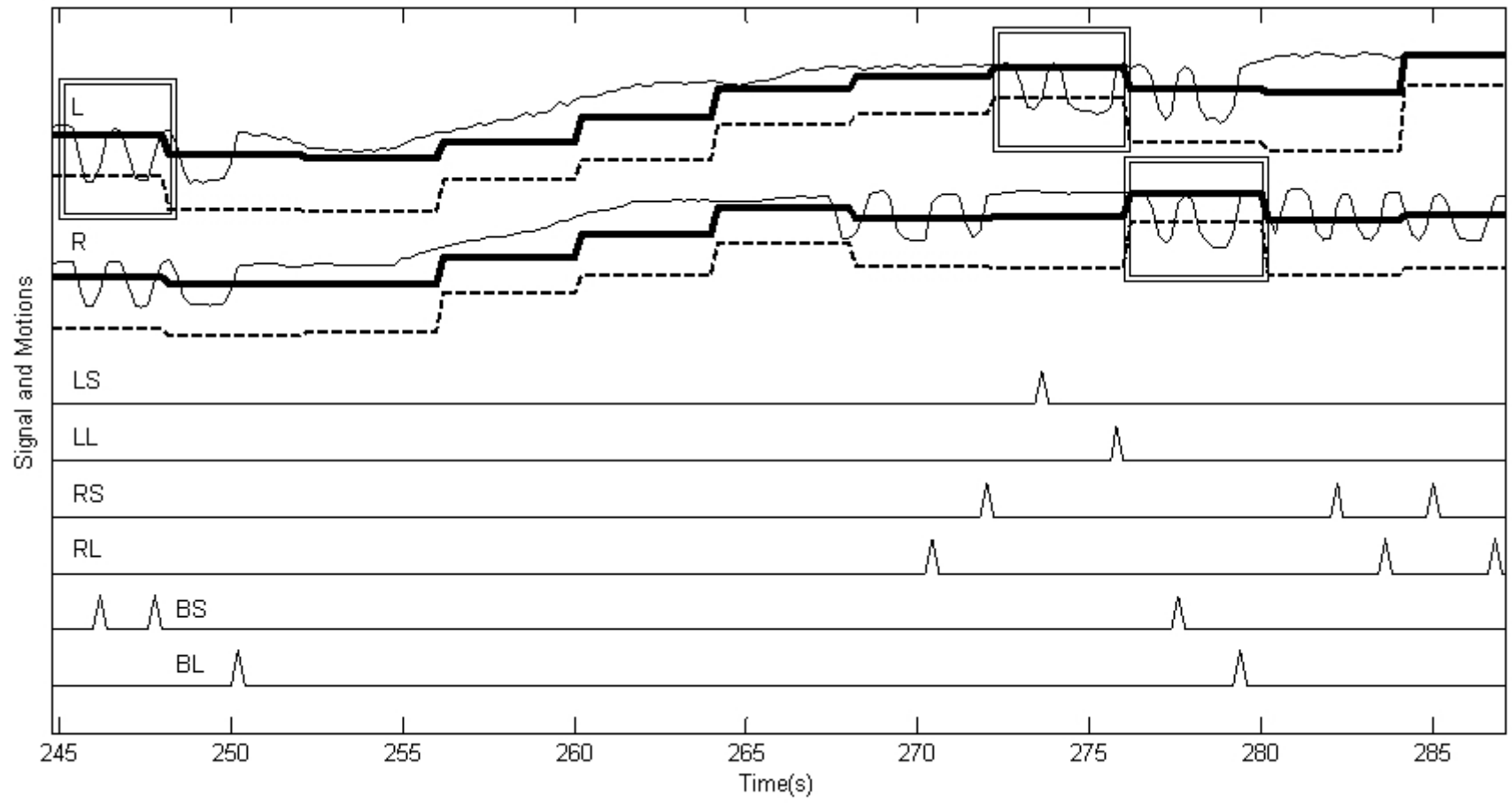


Figure 4-4 Illustration of the threshold value adjustment

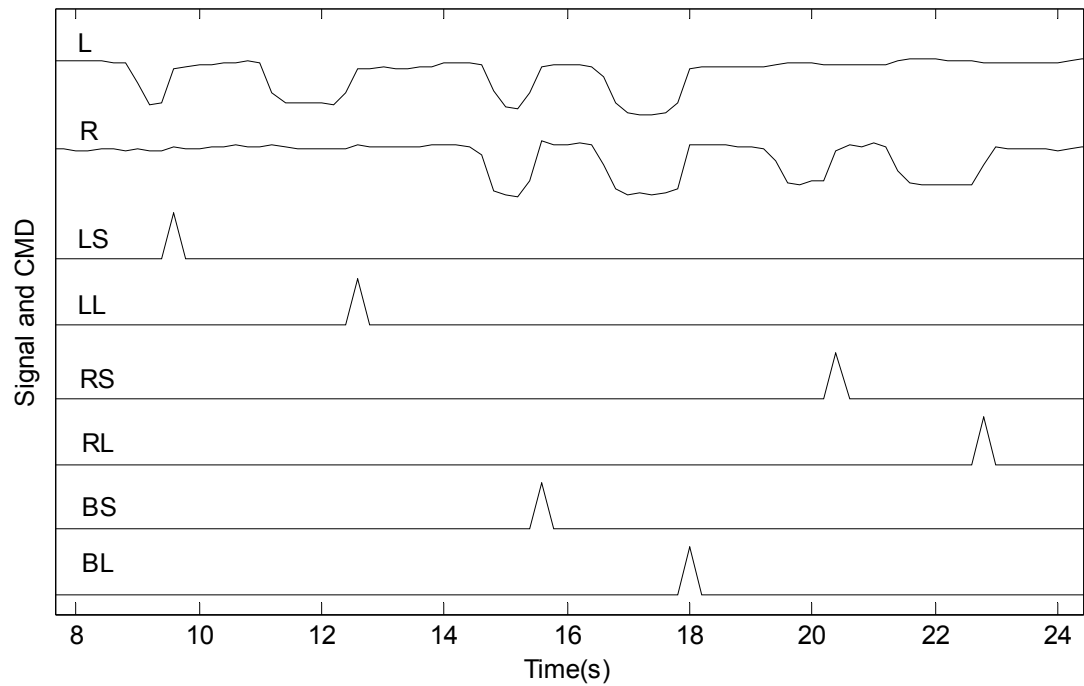


Figure 4-5 Bioimpedance signal classification result

4.3.2 Overshoot detection

Sometimes, the signal will be interfered by some noise which can make the signal root mean square value change to be many times of the normal signal. In case of wrong operation, we use the inequation (4.4) and (4.5) as a limit of the valuable signal. If the signal meets one of the conditions, the signal will not be used to determine the control command.

$$RMS - RMS_{\max} > X \times (RMS_{\max} - RMS_{\min}) \quad (4.4)$$

$$RMS_{\min} - RMS > X \times (RMS_{\max} - RMS_{\min}) \quad (4.5)$$

where RMS = the resent signal root mean square value, RMS_{\max} and RMS_{\min} are the same in equation (4.1). X = the possibility multiple of the overshoot value to the normal value. In our experiment, it was set to 5.

4.3.3 No movement protection

As a result of auto threshold value adjustment, the system will get some limitation because we use the threshold value of previous period to determine the output command. In this case, there are two situations which the system cannot detect the movement (Figure 4-2, situation B and C):

When there is no any movement for a duration longer than one period of threshold adjust (Figure 4-2, situation B), the threshold value calculated by the auto adjust algorithm is almost the same with the recent signal value;

Hold the same action for a duration which longer than one period of threshold adjustment (Figure 4-2, duration C).

In order to avoid no movement situation that is determined by

$$\text{RMS}_{\max} - \text{RMS}_{\min} > P_n \quad (4.6)$$

where RMS_{\max} and RMS_{\min} are the same in equation (4.1), P_n is a parameter set according to the small change of root mean square value during there is no movement for a long time. The threshold value will be calculated by equation (4.1).

For avoiding the second situation which is determined by

$$\text{RMS}_T < \text{RMS}_{\min} \quad (4.7)$$

where RMS_T and RMS_{\min} are the same in equation (4.1), we are going to calculate the threshold value by

$$\text{RMS}_T = \text{RMS}_{\min} + P_n \quad (4.8)$$

where RMS_T is system threshold value, RMS_{\min} and P_n are the same as in equation (4.5).

4.4. System simulation

We simulated our system on the computer with software LabVIEW 8.2. At first, six LEDs were used to simulate six motions of this system after bioimpedance signal classification. Figure 4-6 shows the led simulation panel. each LED represents a motion. The first row are the short motions, while second are the long motions of left shoulder, both shoulders and right shoulder from left to right respectively. The simulation indicated a 100 percents correct control on the LED. After see the first stage simulation result met out anticipation, we designed second stage simulation. A map was drawn for the virtual wheelchair control simulation with six motions which are get from shoulders movement (up and down). Wheelchair control operation: turn left 30°, turn left 90°, turn right 30°, turn right 90°, turn round 180°, run and stop were applied. Figure 4-7 shows wheelchair control panel. In this simulation, subjects have to get used to the map. Subjects have to follow the wheelchair's direction. They had better image themselves sit on the wheelchair because the direction principle on a virtual environment is different from the traditional direction principle. But if the portable device is made, this problem will not exist anymore. Also, subjects need to familiar with the movement related to the motions. So there will be a training time for them before control the real interface until they can manage the wheelchair control simulation.



Figure 4-6 LED control simulation panel

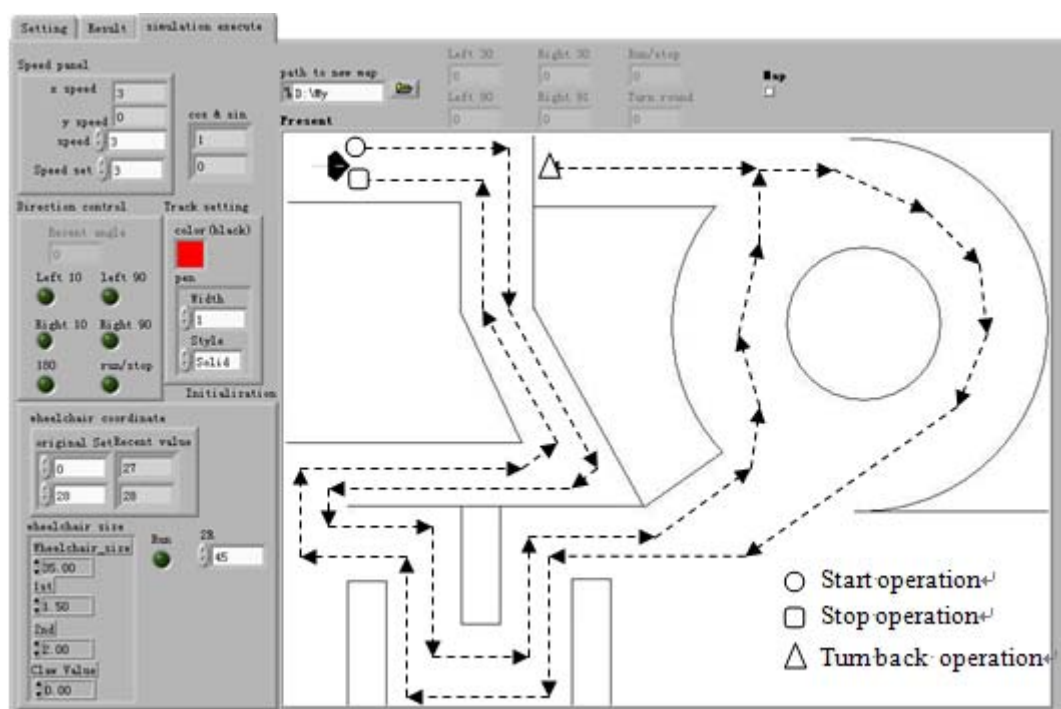


Figure 4-7 Wheelchair control simulation panel

4.5. Evaluation of wheelchair control

The system has been developed and simulated successfully. But there is a necessary to test on some other subjects to evaluate the system to see if the developed interface is practicable and stable. Five volunteers involved in this evaluation: Mr. Huang Yunfei, Mr. Wang Shenming, Mr. Xu Shubing, Mr. Wang Xianwei and Mr. Fu dongJin. Details were shown in Table 3. Column four is the training time for each volunteer until they can manage the control the process from the beginning to the end. It is different during each other. The main reason is to tell the short and long time movement. The other reason is that sometimes they would make a wrong operation owe to the wrong judge of the direction ahead. But it does not matter, because each individual can manage it after a long or short time practice and train. Pictures (Figure A 1, Figure A 2, Figure A 3, Figure A 4, Figure A 5) in appendix II shows the volunteers photograph and their five simulation tracks respectively. Their simulation videos are included in the appendix CD.

Table 3 Evaluation subject detail description

	Name	Weight (kg)	Height (cm)	Age (y)	Training time (hour)
1	Huang Yunfei	70	173	24	designer
2	Wang Shenming	50	163	23	1.5
3	Xu shubing	48	166	24	2.5
4	Wang Xianwei	83	182	25	2
5	Fu Dongjin	57	168	24	3

4.6. Conclusion

Firstly, electrodes configuration and motion design are introduced. We adopt three electrodes to make up 2 signal acquisition channels which is based on the four electrodes method. Through this electrodes configuration, in addition with the

bioimpedance characteristic which it is proportional to the movement, we can achieve six kind of motions: left shoulder short time motion, left shoulder long time motion, right shoulder short time motion, right shoulder long time motion, both shoulder together short time motion and both shoulder together long time motion. Use those motions it's easy to design a command system for the wheelchair control. Secondly, it describes the detail of all the periods which are existing in the control duration. In the third section, it is a section for the software design and motion classification. It shows the software structure with a block diagram, shows the process of signal classification and the process that the threshold value is adjusted automatically. Classification results which are according to our design and desire are presented. In section four, the LED control simulation and the wheelchair control simulation are described. In section five, it presents results of the evaluation with five volunteers completing the wheelchair control simulation mission. It demonstrates the practicability and stability of the human device interface based on bioimpedance.

Chapter 5. Summary

5.1. Conclusion

The principle of frequency selection is based on the frequency characteristic of the Cole-Cole system (segment tissue). The frequency which caused the highest bioimpedance change at the same electrode configuration will be chosen. From the literature review, the frequency of current used by the researchers are 50 kHz [3][4][5][6][16][17] and 75 kHz [14][15]. In order to find out the optimal frequency for our project, we tested frequency from 1 kHz~200 kHz at shoulders, finally, the optimal frequency was found: 50 kHz, which was applied in our system.

For the current magnitude chosen, things we have to think about are: not hurt the user, save power, and easy to detect the movement. The previous researchers have chosen 300 μ A [3][4][5][6], 500 μ A [16][17], 1 mA [14] and 3.8 mA [15], all of them are acceptable, and we use 300 μ A in our project.

NI (National Instrument) productions are good solutions at the developing and modeling phase of a product. It is so easy to realize data connection and analysis if using the data acquisition device cooperate with NI LabVIEW software tools. LabVIEW is very convenient to use as they make every function a module, even people who do not have any program language background can master to use after short time training. In our study, we adopt LabVIEW 8.2 cooperated with NI PCI 6250 DAQ device to sample the bioimpedance signal. Then all of the work was done on LabVIEW 8.2, include signal processing, classification and simulation.

Because it is not convenient to find the right subject that has been mentioned in the problem statement section, we had only find the healthy subjects whose age range from twenty to thirty. All subjects were request to sit on the chair to fulfill the test. In order to find the performance of the system and to find how easy it works with the operators, five subjects were invited to test this system. Repetitive test

was taken on the same subject five times. Results of at the same subject were compared so that we can see the problems and the reasons that caused the problem.

Impedance property of human tissue offers a promising possibility for detecting the segment movement. This opens an opportunity to enable bioimpedance-based wheelchair control to practical applications. We proposed to develop a novel human machine interface for the wheelchair control. Three electrodes are used to acquire two channels of bioimpedance from the trapezius muscle. Three shoulder movements, i.e. left shoulder up, right shoulder up, and both shoulders up, are used to generate control signals. In addition, bioimpedance almost can be considered as the kinematic information. Its change follows the segment movement. Therefore, it is possible to keep the change of impedance signal for certain duration. We make use of the time characteristic of bioimpedance to make more motions, i.e. short action ($300 \text{ ms} < T_{\text{hold}} < 1000 \text{ ms}$) and long action ($T_{\text{hold}} > 1000 \text{ ms}$). As a result, six operation capabilities for wheelchair control are feasible. At first, the proposed system was evaluated by controlling LED on a computer. Results show that 100% accuracy is obtained. Secondly, wheelchair control simulation was the found on the classified six motions. As a result, the wheelchair can be controlled easily.

5.2. Recommendations for future work

Firstly, as the scope of the study has limitation. The future works are recommended. All of the experiment was test on the healthy subjects as it is easy to find. However, the test result did not give any suggestion that it can work well with the person who is the potential user of this system. The effect on them should be some differences compared with the expected result, therefore, to find the real disabled people who possibly have the requirement to participate in this research are necessary. To let them to be trained, to let them practice and to get comments from them so that we can find the blind site and improve it. We also can modify the function of our interface depend on their desire. Those works will perfect the system.

Secondly, this is a human device interface which is based on the bioimpedance. We have made a full use of the right characteristic (bioimpedance is almost linear proportional to the movement). It helped us gain three more motions which divide the motion into short time and long time motions according to the duration of the action hold. Even though, it was just used as an on-off variable. But actually this characteristic can be more deeply used.

Bioimpedance can be used to evaluate the athlete's skill cooperated with surface EMG signal, which will be more accuracy and efficient. Because the surface EMG signals just come up at the beginning of the movement while the bioimpedance change can follow with each phase of the movement from the beginning to the end.

So, if surface EMG signals are recorded commands, each command stand for a single start movement while a serial of them can show the whole movement sequence. Recording all bioimpedance signals, we can watch the quality of each moment of the whole procedure for a full movement. We can compare our clues' data to the perfect one. It will help the coach to find the problem of the athletes more easily and find the solution and train scenario.

References

- [1] T. Guerreiro and J. Jorge, "Assistive technologies for spinal cord injured individuals: Electromyographic mobile accessibility," *Proceedings of GW 2007, 7th International Workshop on Gesture in Human-Computer Interaction and Simulation*, Lisbon, Portugal, May 2007.
- [2] M. A. Oskoei and H. Hu, "Review myoelectric control systems—A survey," *Biomedical Signal Processing and Control*, Vol.2, pp. 275-294, September 2007. [Online]. Available: <http://www.sciencedirect.com>. [Accessed June 12, 2008].
- [3] K. S. Kim, D. Y. Yoom, Y. K. Yang, J. H. Seo, K. S. Kim, and C. G. Song, "a new bioimpedance sensor technique for leg movement analysis," *Proceedings of Intelligent Sensors, Sensor Networks and Information Processing Conference*, pp. 487-490, 2004.
- [4] J. C. Kim, S. C. Kim, K. C. Nam, S. H. Ahn, M. Park, and D. W. Kim, "Evaluation of a bioimpedance method for measuring human arm movement," *Yonsei Medical Journal*, vol. 43(5), pp. 637-645, 2002.
- [5] S. C. Kim, K. C. Nam, D. W. Kim, C. Y. Ryu, Y. H. Kim, and J. C. Kim, "Optimum electrode configuration for detection of arm movement using bioimpedance," *Medical & Biological Engineering & Computing*, vol. 41, pp. 141-145, 2003.
- [6] C. G. Song, S. C. Kim, K. C. Nam, and D. W. Kim, "Optimum electrode configuration for detection of leg movement using bioimpedance," *Physiological Measurement*, vol. 26 (issue 2), pp. 59-68, April 2005.
- [7] K. Choi and M. Sato, "A new human-centered wheelchair system controlled by the EMG signal," *Proceeding of the World Congress on Computational Intelligence*, Vancouver, Canada, 2006.
- [8] J. S. Han, Z. Z. Bien, D. J. Kim, H. E. Lee, and J. S. Kim, "Human-machine interface for wheelchair control with EMG and its evaluation," *Proceedings of the 25th Annual International Conference of the Engineering in Medicine and Biology Society (IEEE-EMBS 2003)*, pp. 1602-1605, Cancun, Mexico, 2003.
- [9] I. Moon, M. Lee, J. Chu, and M. Mun, "Wearable EMG-based HCI for electric-powered wheelchair users with motor disabilities," *Proceedings of IEEE*

- International Conference on Robotics and Automation*, pp.2660-5, Barcelona, Spain, 2005.
- [10]C. S. L.Tsui, P. Jia, J. Q. Gan, H. Hu, and K. Yuan, “EMG-based hands-free wheelchair control with EOG attention shift detection,” *Proceedings of IEEE International Conference on Robotics and Biomimetics (ROBIO2007)*, pp. 1266-1271, Sanya, China, 2007.
- [11]J.-M. I Maarek and L. Ward, “Bioimpedance,” wikipedia.org, para.1, 2, February. 25, 2008. [Online]. Available: <http://en.wikipedia.org/wiki/Bioimpedance>. [Accessed: July. 12, 2008].
- [12]L. E. Baker, “Principles of the impedance techniques,” *IEEE Engineering in Medicine and Biology Magazine*, Vol. 8 (issue 1), pp. 11-15, March 1989.
- [13]I. Moon, M. Lee, and M. Mun, “A novel EMG-based human-computer interface for persons with disability,” *Proceedings of the IEEE International Conference, Mechatronics, 2004, ICM '04*, pp.519–524, June 2004.
- [14]S. Papezova, “Signal processing of bioimpedance equipment,” *Sensors and Actuators B: Chemical*, Vol.95, No.1, pp.328–335, October 2003.
- [15]M. Collette, A. Humeau, and P. Abraham, “Time and spatial invariance of impedance signals in limbs of healthy subjects by time-frequency analysis,” *Annals of Biomedical Engineering*, Vol. 36, No. 3, pp. 444-451, March 2008.
- [16]Y. Yamamoto, T. Nakamura, T. Kusuhara, and Adli, “Consideration of conditions required for multi-channel simultaneous bioimpedance measurement,” *Proceedings of the IEEE Instrumentation and Measurement Technology Conference*, pp. 231-234, Minnesota, USA, May 1998.
- [17]T. Nakamura, Y. Yamamoto, T. Yamamoto and H.Tsuji, "Fundamental characteristics of human limb electrical impedance for biodynamic analysis," *Medical & Biological Engineering & Computing*, vol. 30, pp. 465-473, 1992.
- [18]S. J. Grimnes, O. G. Martinsen, “Electrodes: design and properties,” *Bioimpedance and Bioelectricity Basics: Instrumentation and Measurement*, 2nd ed., S. Grimnes, ed. Great Britain: 2008, pp.275.
- [19]Y. F. Huang, P. Phukpattaranont, B. Wongkittisuksa, and S. Tanthanuch, “Development of a bioimpedance-based human machine interface for wheelchair

- control,” *Proceedings of the ECTI International Conference (ECTI-CON 2009)*, pp. 1032–1035, Pattaya, Thailand, May 2009.
- [20] Y. F. Huang, P. Phukpattaranont, B. Wongkittisuksa, and S. Tanthanuch, “A novel design and development on bioimpedance-based wheelchair control,” *Proceedings of the 3rd International Convention on Rehabilitation Engineering & Assistive Technology (i-CREATe 2009)*, pp. 17–20, Singapore, April 2009.
- [21] Y. F. Huang, P. Phukpattaranont, S. Tanthanuch, K. Chetpatananondh, B. Wongkittisuksa, and C. Limsakul, “Evaluation of human machine interface for wheelchair control with bioimpedance,” *Proceedings of the 24th Japanese Conference on the Advancement of Assistive and Rehabilitation Technology (the 24th JCAART)*, pp. 227–228, Japan, August 2009.

Appendix

Appendix I. Published papers

Development of a bioimpedance-based human machine interface for wheelchair control

Huang Yunfei¹, Pornchai Phukpattaranont², Booncharoen Wongkittisuksa³, Sawit Tanthanuch⁴
^{1,2,3,4}Department of Electrical Engineering, Faculty of Engineering, Prince of Songkla University, Thailand
¹*Crazy-chinese-boy@hotmail.com*, ²*pornchai.p@psu.ac.th*

Abstract—We present a new method, which is based on bioelectrical impedance of the trapezius muscles, to control wheelchair for the disabled people and the elderly. In our application, three electrodes were used for detecting the changes in movements of left and right trapezius muscles. The modified Howland current bridge supplies the 0.5 mA ac current for the measure system at the frequency of 50 kHz. NI PCI-6250 DAQ board were adopted to collect the data and Labview8.2 was used to implement the control system. The threshold value in detection algorithms applied in the system is automatically adjusted to the change in the measured signal magnitude. Pump value detection is used to detect an unexpected large change of the signal to avoid the wrong operation. As a result, we can find that the change of the signal according to the movement of the shoulder is very stable. Additionally, after some signal processing we can use shoulder movement to control LED on Labview8.2 with an accuracy of 100%.

I. INTRODUCTION

Recently, a large amount of rehabilitative devices is required by many populations who have diseases such as myelopathy, upper limb disabled, lower arm disabled, loss of skeletal muscle control from below the shoulders, and hand amputees. The limitations imposed by these diseases deprive the injured individuals from operating electronic devices. Besides the drastic quality of life reduction directly imposed by the impairments, individuals also face a communication shutdown as they are often incapable of operating devices that make possible to communicate with others (computer, cell phone, and PDA etc.). It is a worldwide concern to reconstitute disabled users communicative and control skills to improve their quality of life. Therefore, human machine interface comes with these reasons.

As we know, the main studies in this field are prosthesis and wheelchair. Prosthesis is the most important and only commercial application. However, wheelchair is also a very useful application. In this paper, we focus on human machine interface for disabled people applied on a wheelchair control. There are researchers who studied the EMG-based electric wheelchair control [1]-[4]. However, none of these studies have examined a bioimpedance-based wheelchair control. In our study, we proposed to use the bioimpedance from shoulders to analyze the human movement and develop a hand-free wheelchair control to help the disabled people with the high level spinal cord injury, quadriplegia and others who can not use their hands. In order to complete the basic function

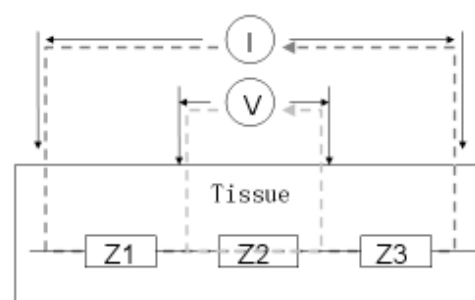


Figure 1. Four-electrode method for bioimpedance measurement.

of the wheelchair operation, four classes of motions are required, i.e. run, stop, turn left, and turn right.

The main characteristics of segment movement analysis using bioimpedance are as follows:

- 1) When we excite a constant current, the bioimpedance change between the measuring electrodes is directly proportional to the intensity of segment movement.
- 2) Bioimpedance signals are time and spatial invariant on a given segment of limbs and the chest for healthy subjects at rest [5].
- 3) Bioimpedance almost can be considered as the kinematic information because its change follows the segment movement [6].

In the recent few years, researchers have started to study the use of bioimpedance on movement analysis [7]-[10].

II. THEORY

A. Four electrodes system

The four electrodes method shown in Figure 1 is a widely accepted technique used to measure the bioimpedance. The four electrodes method uses two electrodes to supply current to the tissue and another two electrodes to measure the bioimpedance. As a result, the bioimpedance z can be calculated by

$$z = \frac{V}{I} \quad (1)$$

where V is the voltage and I is the current.

B. The effective factor of bio-impedance

The human tissue can be seen as the parallel conductor model which consists of muscle and blood. Bioimpedance can be expressed by

$$z = \frac{L}{\sigma_m S_m + \sigma_b S_b} = \frac{L}{\sigma_m S_m + \sigma_b V_b / L} \quad (2)$$

where σ_m is conductivity of muscle, σ_b is conductivity of blood, S_m is sectional area of muscular tissue, S_b is sectional area of blood vessel, L is length of measured part, and V_b is volume of blood. Because L , σ_m , and σ_b are almost constant, bioimpedance is mainly determined by V_b and S_m [6]. It is reasonable that the change in bioimpedance is proportional to the movement.

III. MATERIALS AND METHODS

A. Measure system configuration

Figure 2 shows the block diagram of bioimpedance measurement for the control system. Voltage to current converter circuit converted the 50 kHz signal generated by a function generator to 0.5 mA ac current. Then, this current was injected to human tissue. NI PCI-6250 DAQ board was used to acquire the data at a sampling frequency of 600 kHz for each channel. The signal was stored and then processed with Labview8.2 software. Finally, we used the classified signal to control LEDs on labview8.2 software simulating the wheelchair control.

B. Electrodes configuration and motion design

The disabled people such as spinal cord injury, myelopathy, upper limb disabled, lower arm disabled, loss of skeletal muscle control from below the shoulders and hand amputees, cannot use their hands to operate the wheelchair. We need to design the electrodes location so that these populations are

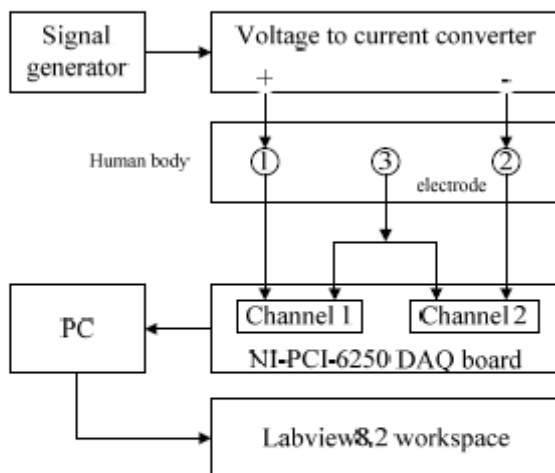


Figure 2. Block diagram of the bioimpedance measurement for the control system.

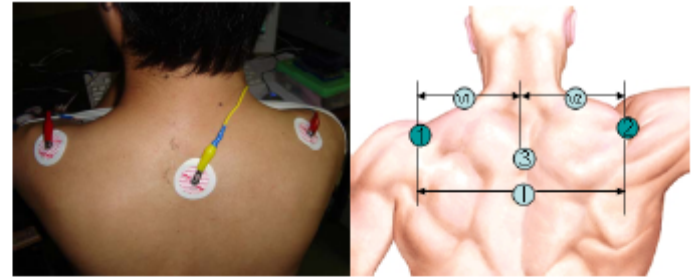


Figure 3. Electrodes configuration.

convenient to operate. As a result, the locations on the trapezius muscle are chosen as shown in Figure 3. For two channels, three electrodes were used. Electrode number 1 and 2 were used to supply the current to the tissue. Moreover, each of them also is one of the voltage detecting electrodes for a certain channel. Electrode number 3 is the common end of the two channels.

Four motions, i.e. run, stop, turn left and turn right, are designed for wheelchair operation. The design of motions related to the segment of human body is shown in TABLE I. In addition, TABLE II shows details description of the motions. It tells how motions transfer from one state to another state.

C. Bioimpedance classification algorithm

The control system was implemented on the Labview8.2 work space. Figure 4 is the block diagram of Labview8.2 program for the control system in our project. First, 50000 raw bioimpedance signals were collected through NI PCI-6250 DAQ board in real time. Second, the signal was filtered by

TABLE I
WHEELCHAIR MOTION DESIGN

Electrodes' No.	Muscle	Segment	Motion
1,3	Left trapezius muscle	Left shoulder	Left
2,3	Right trapezius muscle	Right shoulder	Right
(1,3) and (2,3)	Left and right trapezius muscle	Left and right shoulder	Stop/Run

TABLE II
THE MOTION DESCRIPTION OF THE INTERFACE

Motion No.	Operation	Description
1	Turn left	Left shoulder up and down
2	Turn right	Right shoulder up and down
3	Stop / run	Both shoulders up and down

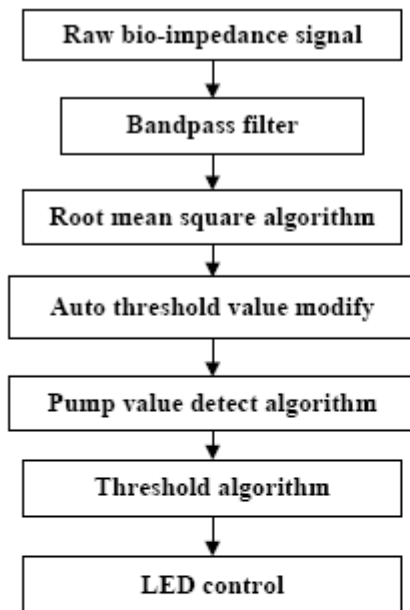


Figure 4. Block diagram of Labview8.2 program for the control system.

a bandpass filter at the 49 kHz low cutoff frequency and 51 kHz high cutoff frequency. Third, we calculated the root mean square value of the 50000 filtered signals. Fourth, the system adjusts the threshold value automatically. After the pump value was checked, we compare the current RMS signal value with the threshold value to determine the command type.

1) Auto threshold value adjustment.

The system modifies the threshold value every 50 RMS values (RMS value is calculated by 50000 signal sample) because the magnitude of the measured signal sometimes completely changes. The way to find the new threshold value is to store 50 RMS values in an array. Then, the threshold value can be calculated by

$$RMS_{Threshold} = (RMS_{max} + RMS_{min}) / P_{sensitive} \quad (3)$$

where RMS_{max} is the maximal RMS signal value in the array, RMS_{min} is the minimal RMS signal value in the array, $P_{sensitive}$ is the control sensitivity parameter for the control system. $P_{sensitive}$ is a very important parameter. It keeps the balance between the high facility of control and the low error rate of operation. It must be modified manually after:

- Subject change
- And/or electrode position change (not configuration change).

This is due to the fact that the changes in bioimpedance value vary individually. Even on the same subject, when the electrodes are attached at different time, the change in bioimpedance is also different.

2) Pump value detection.

Sometimes, the signal is interfered by some noise, which can make the signal RMS value change pump to be many

times of the normal signal. In case of wrong operation, we use the equation (4) and (5) as a limitation of the signal value. If the signal meets one of the conditions, it is not used to determine the control command.

$$RMS - RMS_{max} > X * (RMS_{max} - RMS_{min}) \quad (4)$$

$$RMS_{min} - RMS > X * (RMS_{max} - RMS_{min}) \quad (5)$$

where RMS is the current signal RMS value, RMS_{max} and RMS_{min} are the same as in equation (3). X is the possibility times of the pump value to the normal value. In our experiment, it was 5.

IV. RESULTS

In the experiment, we implement the control system on the Labview8.2 work space and save the data at the same time. In our application, the signal magnitude change is enough to execute the control task. Therefore, it is not necessary to calculate the real bioimpedance value. As the frequency of our current source is 50 kHz, we designed a FIR bandpass filter (first cutoff frequency at 49 kHz and second cutoff frequency at 51kHz.) to filter the noises, i.e. (power line noise and dc noise. We use power spectral density (PSD) to analyze the frequency component in the signal. Figure 5 shows the original and filtered signal PSD of the measured bioimpedance signal from the shoulder. As we can see, the main noise appeared is the power line noise, and after filter, the frequency power of the filtered signal is mainly focused at 50 kHz.

Figure 6 shows the RMS value and classified control command of the filtered bioimpedance signal from both shoulders. It includes all of the movement: left shoulder up and down; right shoulder up and down; both shoulders up and down. From this figure, we can easily identify the shoulder movement from the RMS value by our eyes. Obviously, the classified control command followed the shoulder movement. In addition, we can use shoulder movement to control LED on Labview8.2 with an accuracy of 100%.

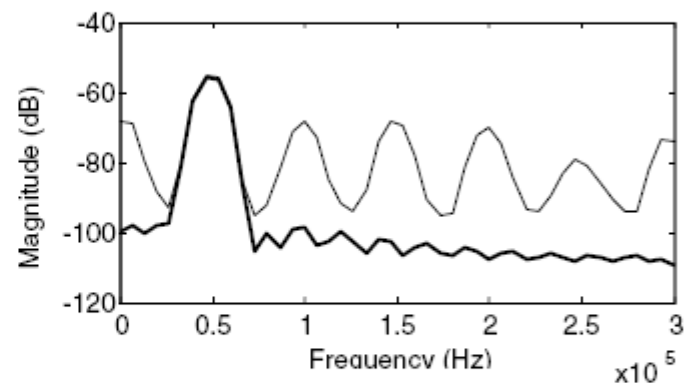


Figure 5. The original and filtered signal PSD of the measured bioimpedance signal from the shoulder. Line in size=1 is the PSD graph of original signal; line in size=2 is the PSD graph of filtered signal.

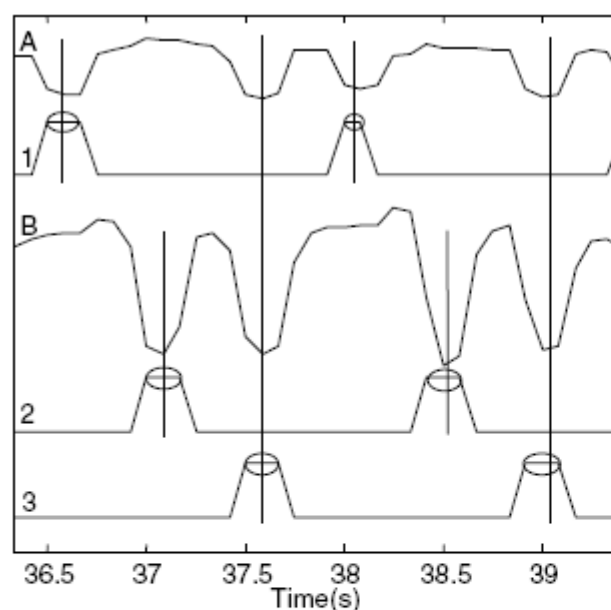


Figure 6. The RMS value of the filtered bioimpedance signal of shoulders.
 Line A: The RMS value of filtered bioimpedance signal from left shoulder.
 Line 1: Left shoulder up and down (Motion No. 1).
 Line B: The RMS value of filtered bioimpedance signal from right shoulder.
 Line 2: Right shoulder up and down (Motion No. 2).
 Line 3: Both shoulders up and down (Motion No. 3).

V. CONCLUSIONS AND DISCUSSION

Impedance property of human tissue offers a high possibility to detect the movement of human body segment. It will make interface based on the bioimpedance feasible in practical applications. In our study, we proposed to develop a new human machine interface for the wheelchair control. The new three electrode configuration works very well. It also can be applied with other segments of human body. We utilized 50 kHz current source in our system, which used by the former researchers. The constant current at this frequency flows almost throughout the tissue of muscle and blood [11]. Even this frequency performs well in our experiment, but we still

doubt about it whether maybe some other frequency will be more suitable for the movement detection. We will make it clear in the future work.

ACKNOWLEDGMENT

This work is supported by NECTEC-PSU center of excellence for rehabilitation engineering and Faculty of Engineering, Prince of Songkla University.

REFERENCES

- [1] K. Choi and M. Sato, "A new human-centered wheelchair system controlled by the EMG signal," in *Int. Joint Conf. on Neural Networks*, 2006.
- [2] J. S. Han, Z. Z. Bien, D. J. Kim, H. E. Lee, and J. S. Kim, "Human-machine interface for wheelchair control with EMG and its evaluation," in *Proc. EMBS 2003*, pp. 1602-1605.
- [3] I. Moon, M. Lee, J. Chu, and M. Mun, "Wearable EMG-based HCI for electric-powered wheelchair users with motor disabilities," in *Int. Conf. Robotics and Automation Proc. 2005 IEEE*.
- [4] C. S. L. Tsui, P. Jia, J. Q. Gan, H. Hu, and K. Yuan, "EMG-based hands-free wheelchair control with EOG attention shift detection," in *IEEE Int. Conf. Robotics and Biomimetics (ROBIO2007)*, Sanya, China, pp. 1266-1271.
- [5] M. Collette, A. Humeau, and P. Abraham, "Time and spatial invariance of impedance signals in limbs of healthy subjects by time-frequency analysis," *Annals of Biomedical Engineering*, Vol. 36, No. 3, pp. 444-451, Mar. 2008.
- [6] T. Nakamura, Y. Yamamoto, T. Yamamoto and H. Tsuji, "Fundamental characteristics of human limb electrical impedance for biodynamic analysis," *Med. Biol. Eng. & Comput.*, vol. 30, pp. 465-473, 1992.
- [7] K. S. Kim, D. Y. Yoom, Y. K. Yang, J. H. Seo, K. S. Kim, and C. G. Song, "A new bio-impedance sensor technique for leg movement analysis," in *2005 IEEE Intelligent Sensors, Sensor Networks and Information Processing Conf.*, pp. 478-490.
- [8] J. C. Kim, S. C. Kim, K. C. Nam, S. H. Ahn, M. Park, and D. W. Kim, "Evaluation of a bio-impedance method for measuring human arm movement," *Yonsei Medical Journal*, vol. 43, no. 5, pp. 637-645, 2002.
- [9] S. C. Kim, K. C. Nam, D. W. Kim, C. Y. Ryu, Y. H. Kim, and J. C. Kim, "Optimum electrode configuration for detection of arm movement using bio-impedance," *Medical & Biological Engineering & Computing*, vol. 41, pp. 141-145, 2003.
- [10] C. G. Song, S. C. Kim, K. C. Nam, and D. W. Kim, "Optimum electrode configuration for detection of leg movement using bio-impedance," *Physiol Meas*, vol. 26, no. 2, pp. 59-68, Apr. 2005.
- [11] L. A. Geddes and L. E. Baker, *Principles of applied biomedical instrumentation*, 3rd ed., New York: Wiley-Interscience, p. 961, 1989.

A Novel Design and Development on Bioimpedance-Based Wheelchair Control

Huang Yunfei, Pornchai Phukpattaranont, Booncharoen Wongkittisuksa, Sawit Tanthanuch
Department of Electrical Engineering, Faculty of Engineering, Prince of Songkla University
Hat Yai, Songkhla, Thailand, 90112

Crazy-chinese-boy@hotmail.com, pornchai.p@psu.ac.th

ABSTRACT

This article presents a novel design and development on bioimpedance-based wheelchair control for the disabled people and the elderly. We use three electrodes to measure two channels of bioimpedance from the trapezius muscle. Bioimpedance changes when there is a movement in the segment of trapezius muscle. We can classify six types of motions resulting in six operation capabilities for wheelchair control based on six types of shoulder movements, i.e. left shoulder up, right shoulder up, and both shoulder up for short time and long time. Our system is composed of the modified Howland current bridge circuit, which supplies the 0.5 mA ac current to the measurement system at the frequency of 50 kHz. NI PCI-6250 DAQ board was adopted to collect the data and Labview 8.2 was used to implement the signal processing and control system. Algorithms applied in the system are an automatic threshold value adjustment, which adapt its value to the measured signal. Pump value detection is used to detect the unexpected large change of the signal to avoid the wrong operation. Results indicate that the change of signal according to the shoulder movement is very stable. Moreover, we can use the shoulder movement to control LED on Labview8.2 with an accuracy of 100%.

Categories and Subject Descriptors

C.3 [Special-purpose and application-based systems]: *Signal processing systems*

General Terms

Algorithms, Design, Experimental.

Keywords

Bioimpedance, wheelchair, motion design, shoulder movement.

1. INTRODUCTION

Recently, a large amount of rehabilitative devices is required by many populations who have diseases such as myelopathy, upper limb disabled, lower arm disabled, loss of skeletal muscle control

from below the shoulders, and hand amputees. The limitations imposed by these diseases deprive the injured individuals from operating electronic devices. Besides the drastic quality of life reduction directly imposed by the impairments, individuals also face a communication shutdown as they are often incapable of operating devices that make possible to communicate with others (computer, cell phone, and PDA etc.). It is a worldwide concern to retrain disabled users communicative and control skills to improve their quality of life. Therefore, human machine interface comes with these reasons.

As we know, the main studies in this field are prosthesis and wheelchair. Prosthesis is the most important and is in commercial application. However, wheelchair is also a very useful application. In this paper, we are focusing on human machine interface for disabled people applied on a wheelchair control. There are researchers who studied the EMG-based electric wheelchair control [1]-[4]. In the recent few years, researchers have started to study the use of bioimpedance on movement analysis [7]-[10]. However, none of these studies have examined a bioimpedance-based wheelchair control. In our study, we proposed to use the bioimpedance from shoulders to analyze the human movement and develop a hand-free wheelchair control to help the disabled people with the high level spinal cord injury, quadriplegia and others who can not use their hands. In order to complete the basic function of the wheelchair operation, four classes of motions are required, i.e. run, stop, turn left, and turn right.

The main characteristics of segment movement analysis using bioimpedance are as follows:

- 1) When we excite a constant current, the bioimpedance change between the measuring electrodes is directly proportional to the intensity of segment movement.
- 2) Bioimpedance signals are time and spatial invariant on a given segment of limbs and the chest for healthy subjects at rest [5].
- 3) Bioimpedance almost can be considered as the kinematic information because its change follows the segment movement [6].

2. THEORY

2.1 Four electrodes system

The four electrodes method is a widely accepted technique used to measure the bioimpedance. The four electrodes method uses two electrodes to supply current to the tissue and another two electrodes to measure the bioimpedance. As a result, the bioimpedance z can be calculated by

$$z = \frac{V}{I}, \quad (1)$$

where V is the voltage and I is the current.

2.2 The effective factor of bioimpedance

The human tissue can be seen as the parallel conductor model, which consists of muscle and blood. Bioimpedance can be expressed by

$$z = \frac{L}{\sigma_m S_m + \sigma_b S_b} = \frac{L}{\sigma_m S_m + \sigma_b V_b / L} \quad (2)$$

where σ_m is conductivity of muscle, σ_b is conductivity of blood, S_m is sectional area of muscular tissue, S_b is sectional area of blood vessel, L is length of measured part, and V_b is volume of blood. Because L , σ_m and σ_b are almost constant, bioimpedance is mainly determined by V_b and S_m [6]. It is reasonable that the change in bioimpedance is proportional to the movement.

3. MATERIALS AND METHODS

3.1 Measurement system configuration

Figure 1 shows the block diagram of bioimpedance measurement for the control system. Voltage to current converter circuit converted the 50 kHz signal generated by a function generator to 0.5 mA ac current. Then, this current was injected to human tissue. NI PCI-6250 DAQ board was used to acquire the data at a sampling frequency of 600 kHz for each channel. The signal was stored and then processed with Labview8.2 software. Finally, we used the classified signal to control LEDs on labview8.2 software simulating the wheelchair control.

3.2 Electrodes configuration and motion design

As the disabled people, such as myelopathy, upper limb disabled, lower arm disabled, loss of skeletal muscle control from below the shoulders, and hand amputees, cannot use their hands to operate the wheelchair, it is necessary to design the electrode location to be convenient use by these populations. As a result, the locations on the trapezius muscle are chosen as shown Figure 2. The electrode number 1 and 2 are used to supply the current to the tissue. In addition, each of them also is used as the voltage detecting electrode for a certain channel. Electrode no. 3 is the common end of the two channels.

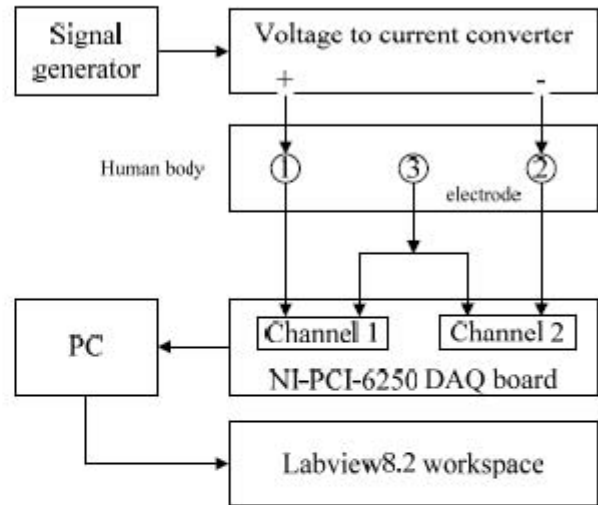


Figure 1. Block diagram of the bioimpedance measurement for the control system.



Figure 2. Electrodes configuration

Although the measurement is based on the four-electrode method, we made some improvement according to our specific application and the specific tissue segment. The conventional four electrodes method needs six electrodes for two channels but we design the new electrode configuration using just three electrodes as shown in Figure 2.

Bioimpedance can be nearly considered as the kinematic information because the bioimpedance change follows the segment movement [6]. This is an advantage of bioimpedance over EMG signal. Therefore, we can achieve more benefit when utilizing bioimpedance as a control signal compared to EMG.

Table 1. Motion design for wheelchair control

Electrodes' No.	Muscle	Segment	Action hold time (T_{hold})	Motion No.
(1,3)	Left trapezius muscle	Left shoulder	$300 \text{ ms} < T_{\text{hold}} < 1000 \text{ ms}$	1
			$T_{\text{hold}} \geq 1000 \text{ ms}$	2
(2,3)	Right trapezius muscle	Right shoulder	$300 \text{ ms} < T_{\text{hold}} < 1000 \text{ ms}$	3
			$T_{\text{hold}} \geq 1000 \text{ ms}$	4
(1,3) and (2,3)	Left and right trapezius muscles	Left and right shoulder	$300 \text{ ms} < T_{\text{hold}} < 1000 \text{ ms}$	5
			$T_{\text{hold}} \geq 1000 \text{ ms}$	6

Table 2. Operation descriptions of motion design

Motion No.	Wheelchair operation	Operation description
1	Turn left 10 degree	If there is a small curve corner, in order to adjust the running direction smoothly during wheelchair running, this command signal makes a 10 degree left side turn.
2	Stop Turn left 90 degree Run	If there is a sharp angle corner, in order to change the direction rapidly, this command signal will control wheelchair to do serial operation: stop, turn left 90 degree, and run.
3	Turn right 10 degree	If there is a small curve corner, in order to adjust the running direction smoothly during wheelchair running, this command signal makes a 10 degree right side turn.
4	Stop Turn right 90 degree Run	If there is a sharp angle corner, in order to change the direction rapidly, this command signal will control wheelchair to do serial operation: stop, turn right 90 degree, and run.
5	Stop/Run (Toggle)	This motion is used to toggle between stop and run the wheelchair.
6	Stop Turn 180 degree	This motion will make the 'turn round' operation conveniently. Command signal will control wheelchair to do the following serial operation: stop and turn left 180 degree.

In our design, two measurement channels of bioimpedance from three electrodes can make six types of motions resulting in six operation capabilities. The design of motions related to the segment and electrode configuration is shown in Table 1. In addition, Table 2 describes the operations related to each design of motions.

3.3 Motion classification algorithm

Motion classification algorithm based on bioimpedance consists of four steps:

1. Collect 50000 raw bioimpedance signals.
2. Filter the collected signals with a bandpass filter at the 49 kHz low cutoff frequency and 51 kHz high cutoff frequency.
3. Calculate the root mean square value of the 50000 filtered signals.
4. Classify motions using automatically adjusted threshold value.

Figure 3 shows the details of motion classification algorithm in the fourth step. Details of the classification algorithm are as follows.

- First, the algorithm will judge if the current root mean square value is a pump value, i.e. an unexpected large change of the signal. If yes, the value cannot be used to determine the command signal and it will be discarded. If no, the current value is kept for classification.
- Second, the algorithm will check if the current period is preceded by a no movement period. If no, the nature threshold value will be the system threshold value. If yes, the no movement period threshold value will be transferred to the system threshold value.
- Third, the system threshold value will be used to compare with the current root mean square signal value to determine the command signal.
- Finally, the duration of the movement will be used to determine the command signal whether is a short period command signal or long period command signal. These

two signals are the final command, which will be used to control the LED on software Labview8.2.

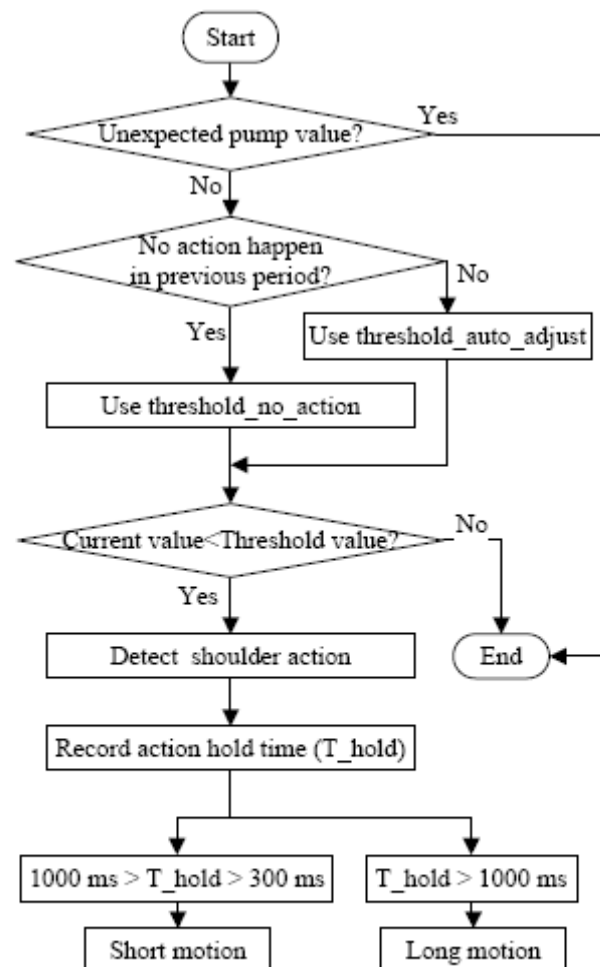


Figure 3. Flow chart of motion classification

4. RESULTS

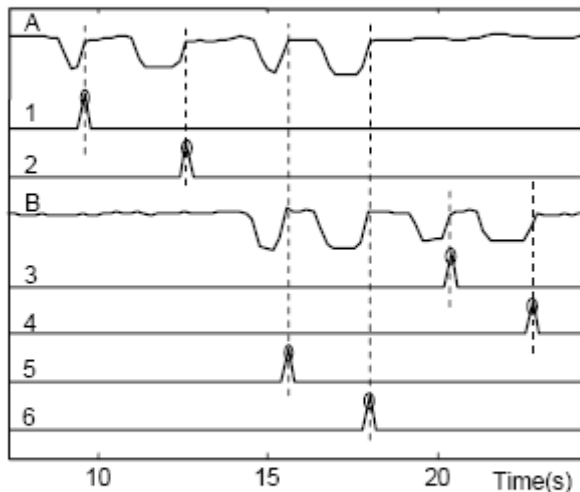


Figure 4. Line A: The RMS value of filtered bioimpedance signal from left shoulder. Line 1: Left shoulder up with short hold time (Motion No. 1). Line 2: Left shoulder up with long hold time (Motion No. 2). Line B: The RMS value of filtered bioimpedance signal from right shoulder. Line 3: Right shoulder up with short hold time (Motion No. 3). Line 4: Right shoulder up with long hold time (Motion No. 4). Line 5: Both shoulders up with short hold time (Motion No. 5). Line 6: Both shoulders up with long hold time (Motion No. 6)

Figure 4 shows the RMS values and the classified control command of filtered bioimpedance signal from six shoulder motions. The numbers (1, 2, 3, 4, 5, 6) placed in Figure 4 are from the motion's number appeared in both Table 1 and Table 2. We can clearly visualize and identify the shoulder movement from the RMS values. Obviously, the classified control command was preceded by the shoulder movement. In addition, we can use the shoulder movement to control LED on Labview8.2 with an accuracy of 100%.

5. CONCLUSIONS AND DISCUSSION

Impedance property of human tissue offers a promising possibility for detecting the segment movement. This opens an opportunity to enable bioimpedance-based wheelchair control to practical applications. We proposed to develop a novel human machine interface for the wheelchair control. Three electrodes are used to acquire two channels of bioimpedance from the trapezius muscle. Three shoulder movements, i.e. left shoulder up, right shoulder up, and both shoulders up, are used to generate control signals. In addition, bioimpedance almost can be considered as the kinematic information. Its change follows the segment movement. Therefore, it is possible to keep the change of impedance signal for certain duration. We make use of the time characteristic of bioimpedance to make more motions, i.e. short action ($300 \text{ ms} < T_{\text{hold}} < 1000 \text{ ms}$) and long action ($T_{\text{hold}} > 1000 \text{ ms}$). As a result, six operation capabilities for wheelchair control are feasible. The proposed system is evaluated by controlling LED on a computer. Results show that 100% accuracy is obtained. Moreover, it is possible to make the proposed system to be a portable device. For example,

the system and algorithm can be implemented in a FPGA chip or a microcontroller. Actually, the classified motion can be implemented in not only for the wheelchair control but also for other devices such as computers and some other portable electronic devices.

6. ACKNOWLEDGMENTS

This work is partially supported by NECTEC-PSU center of excellence for rehabilitation engineering and Faculty of Engineering, Prince of Songkla University.

7. REFERENCES

- [1] Choi, K., and Sato, M. A new human-centered wheelchair system controlled by the EMG signal. In *proceeding of International Joint Conference on Neural Networks, 2006*, 4664-4671.
- [2] Han, J. S., Bien, Z. Z., Kim, D. J., Lee, H. E., and Kim, J. S. Human-machine interface for wheelchair control with EMG and its evaluation. In *proceeding of EMBS 2003*, 1602-1605.
- [3] Moon, I., Lee, M., Chu, J., and Mun, M. Wearable EMG-based HCI for electric-powered wheelchair users with motor disabilities. In *proceeding of International Conference on Robotics and Automation, 2005 IEEE*, 2649-2654.
- [4] Tsui, C. S. L., Jia, P., Gan, J. Q., Hu, H., and Yuan, K. EMG-based hands-free wheelchair control with EOG attention shift detection. In *proceeding of IEEE International Conference on Robotics and Biomimetics (ROBIO2007)*, Sanya, China, 2007, 1266-1271.
- [5] Collette, M., Humeau, A., and Abraham, P. Time and spatial invariance of impedance signals in limbs of healthy subjects by time-frequency analysis, *Annals of Biomedical Engineering*, March 2008, 36(3), 444-451.
- [6] Nakamura, T., Yamamoto, Y., Yamamoto, T., and Tsuji, H. Fundamental characteristics of human limb electrical impedance for biodynamic analysis. *Med. Biol. Eng. & Computing*. 1992, 30, 465-473.
- [7] Kim, K. S., Yoom, D. Y., Yang, Y. K., Seo, J. H., Kim, K. S., and Song, C. G. A new bio-impedance sensor technique for leg movement analysis. In *proceeding of IEEE Intelligent Sensors, Sensor Networks and Information Processing Conference*, December 14, 2005, 487-490.
- [8] Kim, J. C., Kim, S. C., Nam, K. C., Ahn, S. H., Park, M., and Kim, D. W. Evaluation of a bio-impedance method for measuring human arm movement. *Yonsei Medical Journal*, 2002, 43(5), 637-645.
- [9] Kim, S. C., Nam, K. C., Kim, D. W., Ryu, C. Y., Kim, Y. H., and Kim, J. C. Optimum electrode configuration for detection of arm movement using bio-impedance. *Medical & Biological Engineering & Computing*, 2003, 41, 141-145.
- [10] Song, C. G., Kim, S. C., Nam, K. C., and Kim, D. W. Optimum electrode configuration for detection of leg movement using bio-impedance. *Physiological measurement (Physiol Meas)*, April 2005, 26 (2), 59-68.
- [11] Geddes, L. A., and Baker, L. E. *Principles of applied biomedical instrumentation*, (3rd Eds). Wiley-Interscience, New York, 1989, 961.

EVALUATION OF HUMAN MACHINE INTERFACE FOR WHEELCHAIR CONTROL WITH BIOIMPEDANCE

¹Huang Yunfei, ²Pornchai Phukpattaranont, ³Sawit Tanthanuch, ⁴Kanadit Chetpatananondh, ⁴Booncharoen Wongkittisuksa, and ⁴Chusak Limsakul
Department of Electrical Engineering, Prince of Songkla University

1. INTRODUCTION

Recently, a large amount of rehabilitative devices is required by many populations who have diseases such as myelopathy, upper limb disabled, lower arm disabled, loss of skeletal muscle control from below the shoulders, and hand amputees. The limitations imposed by these diseases deprive the injured individuals from operating electronic devices. Besides the drastic quality of life reduction directly imposed by the impairments, individuals also face a communication shutdown as they are often incapable of operating devices that make possible to communicate with others (computer, cell phone, and PDA etc.). It is a worldwide concern subject to retribute disabled users communicative and control skills to improve their quality of life, [1] [2] [3]. We proposed to develop a hand-free wheelchair control to help the disabled people who cannot use their hands. Six operations were obtained from two signal acquisition channels with three electrodes. We achieved a good evaluation of the wheelchair control on Labview8.2 software.

2. THEORY

The four electrodes method is a widely accepted technique used to measure the bioimpedance. The four electrodes method uses two electrodes to supply current to

the tissue and another two electrodes to measure the bioimpedance. As a result, the bioimpedance z can be calculated by

$$z = \frac{V}{I}, \quad (1)$$

where V is the voltage and I is the current.

3. MATERIALS AND METHODS

Measurement system configuration

As shown in Figure 1, Voltage to current converter circuit converted a 50 kHz signal generated by a function generator to 0.5 mA ac current. Then, this current was injected to human tissue (shoulder). NI PCI-6250 DAQ board was used to acquire the data at a sampling frequency of 600 kHz for each channel. The signal was stored and then processed with Labview8.2 software. Finally, we used the classified signal to evaluate the wheelchair control.

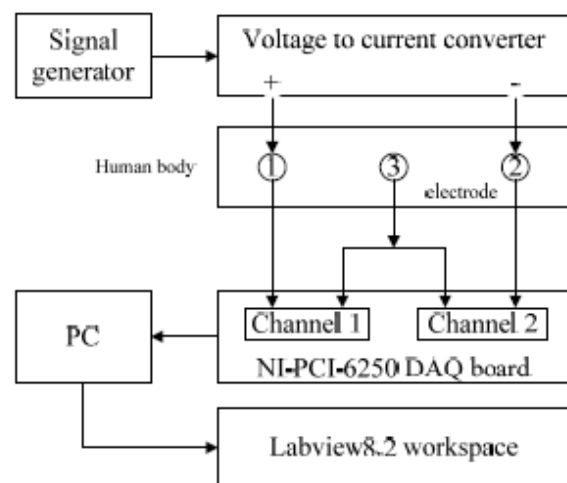


Figure 1. Block diagram of the bioimpedance measurement for the control system.

Electrodes configuration

As the disabled people cannot use their hands to operate the wheelchair, it is necessary to design the electrode location to be convenient use by these populations. As a result, the locations on the trapezius muscle are chosen as shown Figure 2. The electrode number 1 and 2 are used to supply the current to the tissue. In addition, each of them also is used as the voltage detecting electrode for a certain channel. Electrode number 3 is the common end of the two channels.



Figure 2. Electrodes configuration

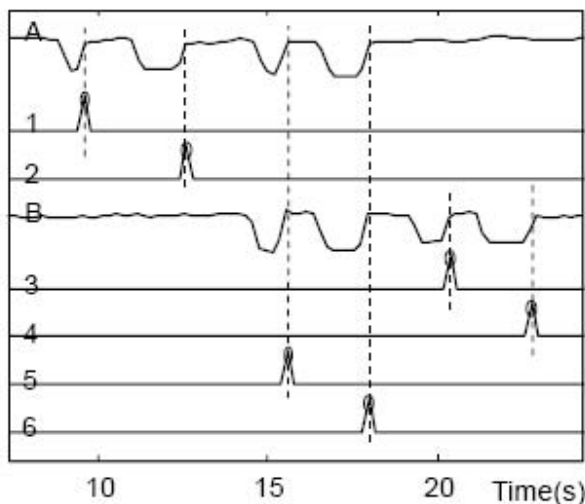


Figure 3. Line A: The RMS value of filtered bioimpedance signal from left shoulder. Line 1: Left shoulder up with short hold time (Motion No. 1). Line 2: Left shoulder up with long hold time (Motion No. 2). Line B: The RMS value of filtered bioimpedance signal from right shoulder. Line 3: Right shoulder up with short hold time (Motion No. 3). Line 4: Right shoulder up with long hold time (Motion No. 4). Line 5: Both shoulders up with short hold time (Motion No. 5). Line 6: Both shoulders up with long hold time (Motion No. 6)

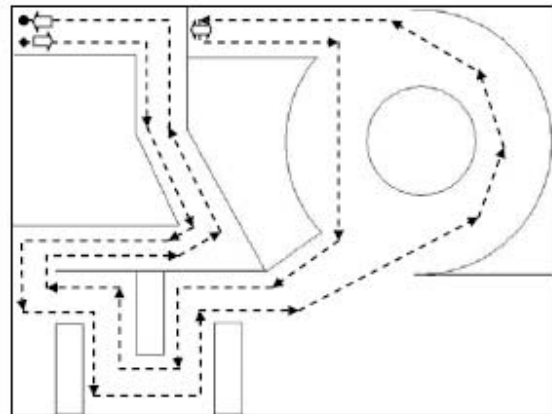


Figure 4. Map for wheelchair control evaluation. Potted line is the expected wheelchair track.

4. RESULTS AND DISCUSSION

Figure 3 shows the RMS values and the classified control command of filtered bioimpedance signal from six shoulder motions. As a result, six operation capabilities for wheelchair control are feasible. The proposed system is evaluated by controlling a model wheelchair on a computer. Results show that we can control the wheelchair smoothly on the complicated map as shown in Figure 4.

5. REFERENCES

- [1] Choi, K., and Sato, M. "A new human-centered wheelchair system controlled by the EMG signal." In *proceeding of International Joint Conference on Neural Networks*, pp. 4664-4671, 2006.
- [2] Han, J. S., Bien, Z. Z., Kim, D. J., Lee, H. E., and Kim, J. S. "Human-machine interface for wheelchair control with EMG and its evaluation," In *proceeding of EMBS 2003*, pp. 1602-1605.
- [3] Moon, I., Lee, M., Chu, J., and Mun, M. "Wearable EMG-based HCI for electric-powered wheelchair users with motor disabilities," In *proceeding of International Conference on Robotics and Automation*, 2005 IEEE, pp. 2649-2654.

Appendix II. Simulation results of volunteers

Appendix II.1. Mr. Huang Yunfei's test result

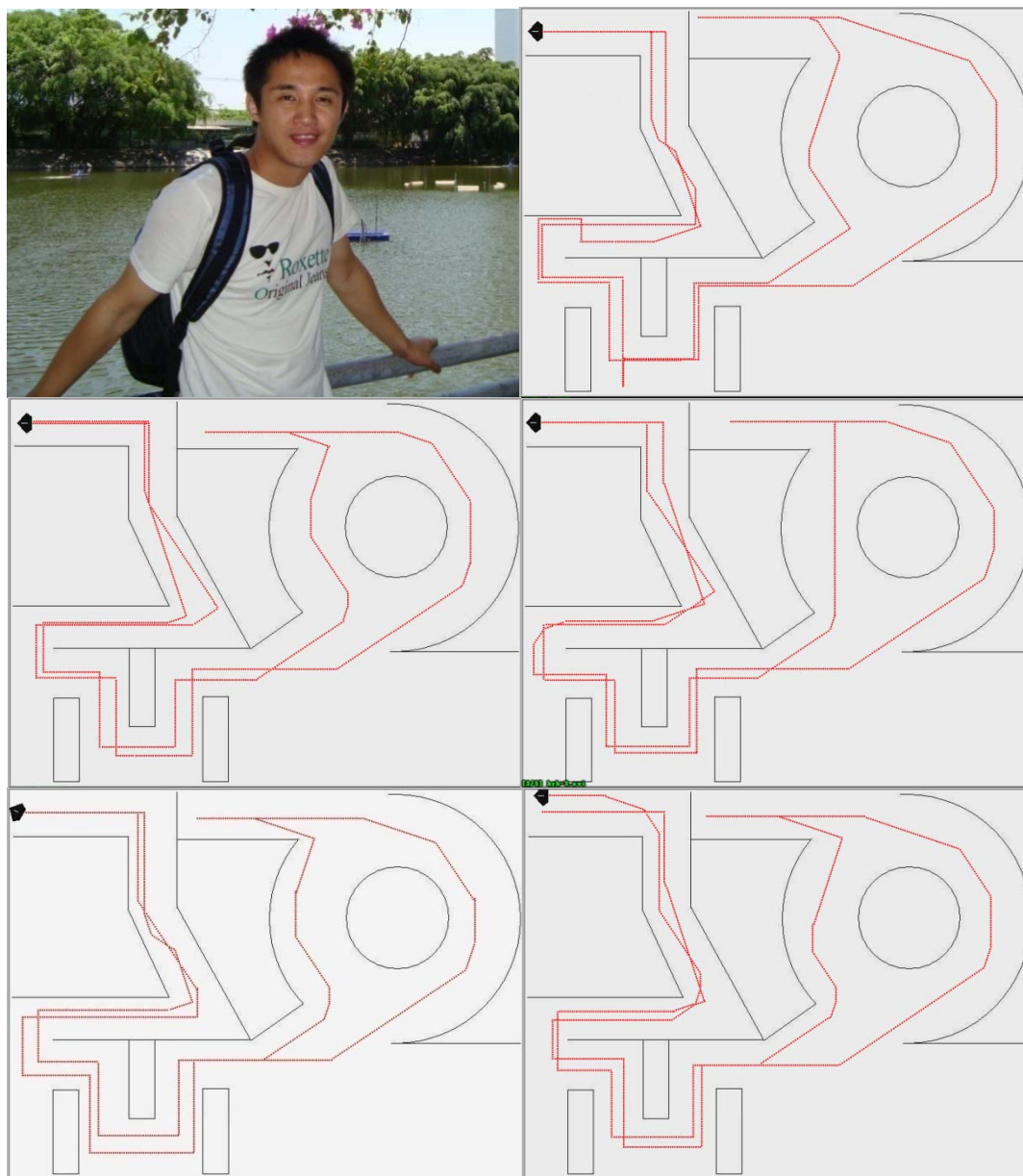


Figure A 1 Mr. Huang Yunfei and his five simulation tracks

Appendix II.2. Mr. Wang Shenming's test result

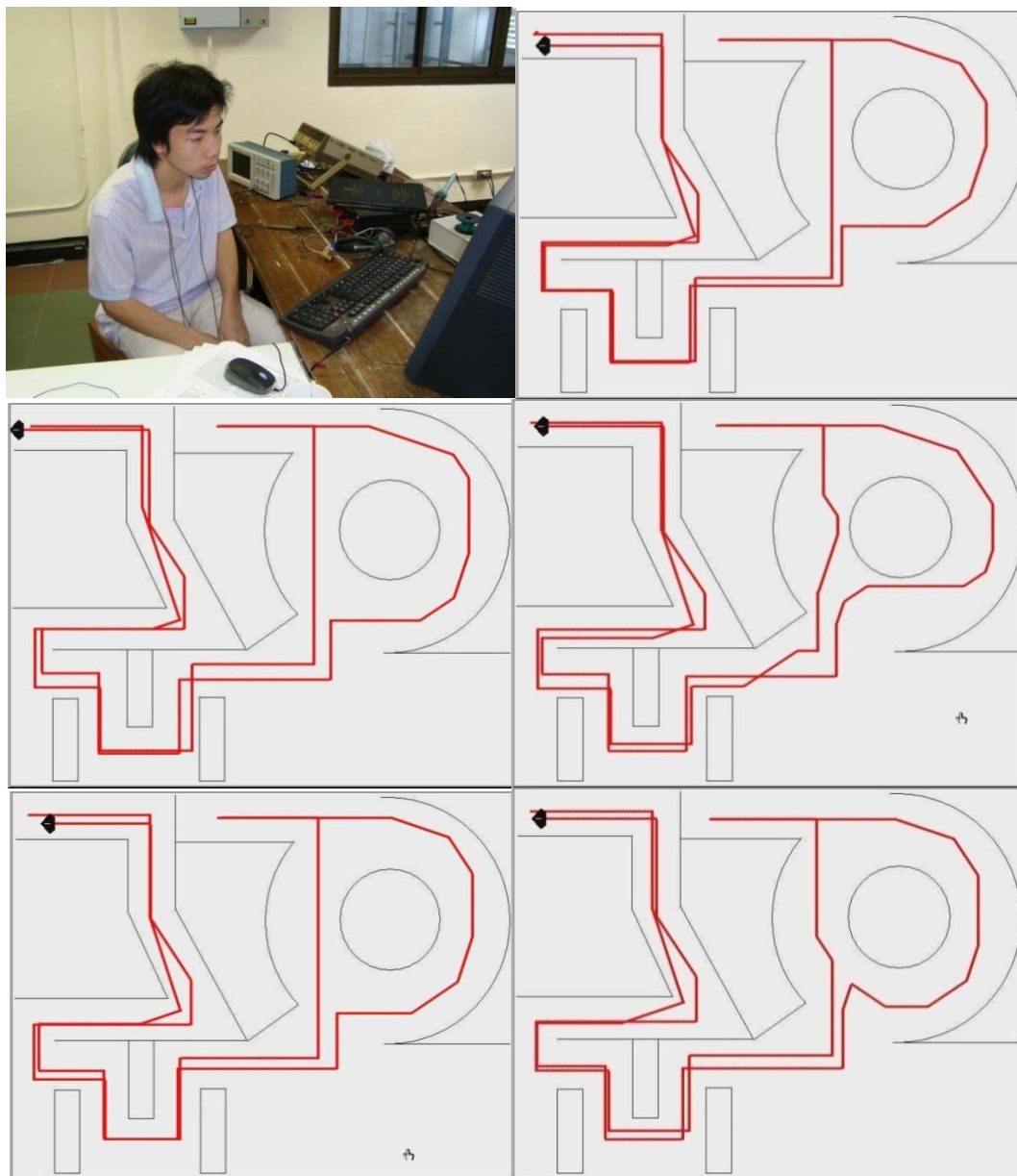


Figure A 2 Mr. Wang Shenming and his five simulation tracks

Appendix II.3. Mr. Xu shubing's test result

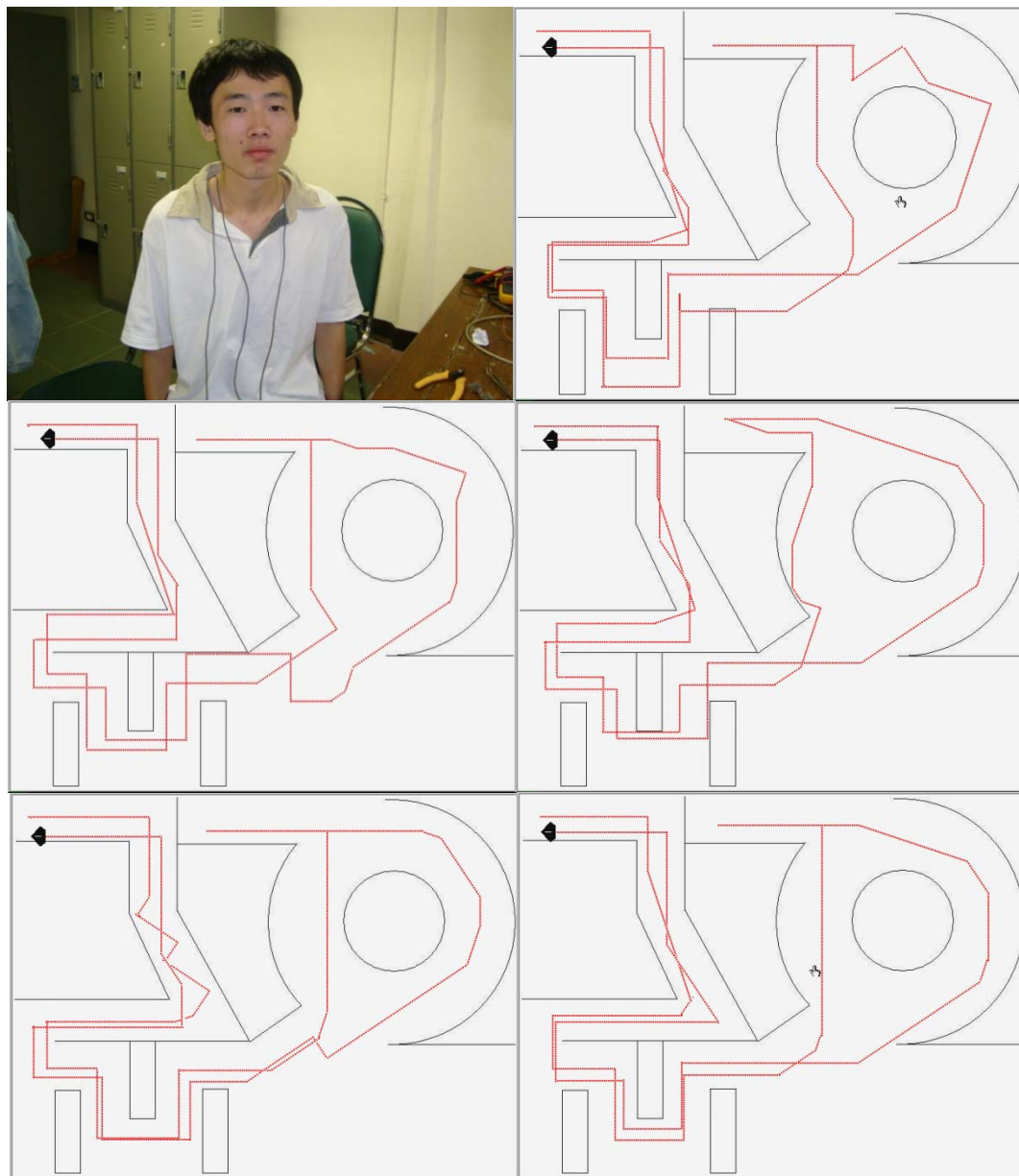


Figure A 3 Mr. Xu Shubing and his five simulation tracks

Appendix II.4. Mr. Wang Xianwei's test result

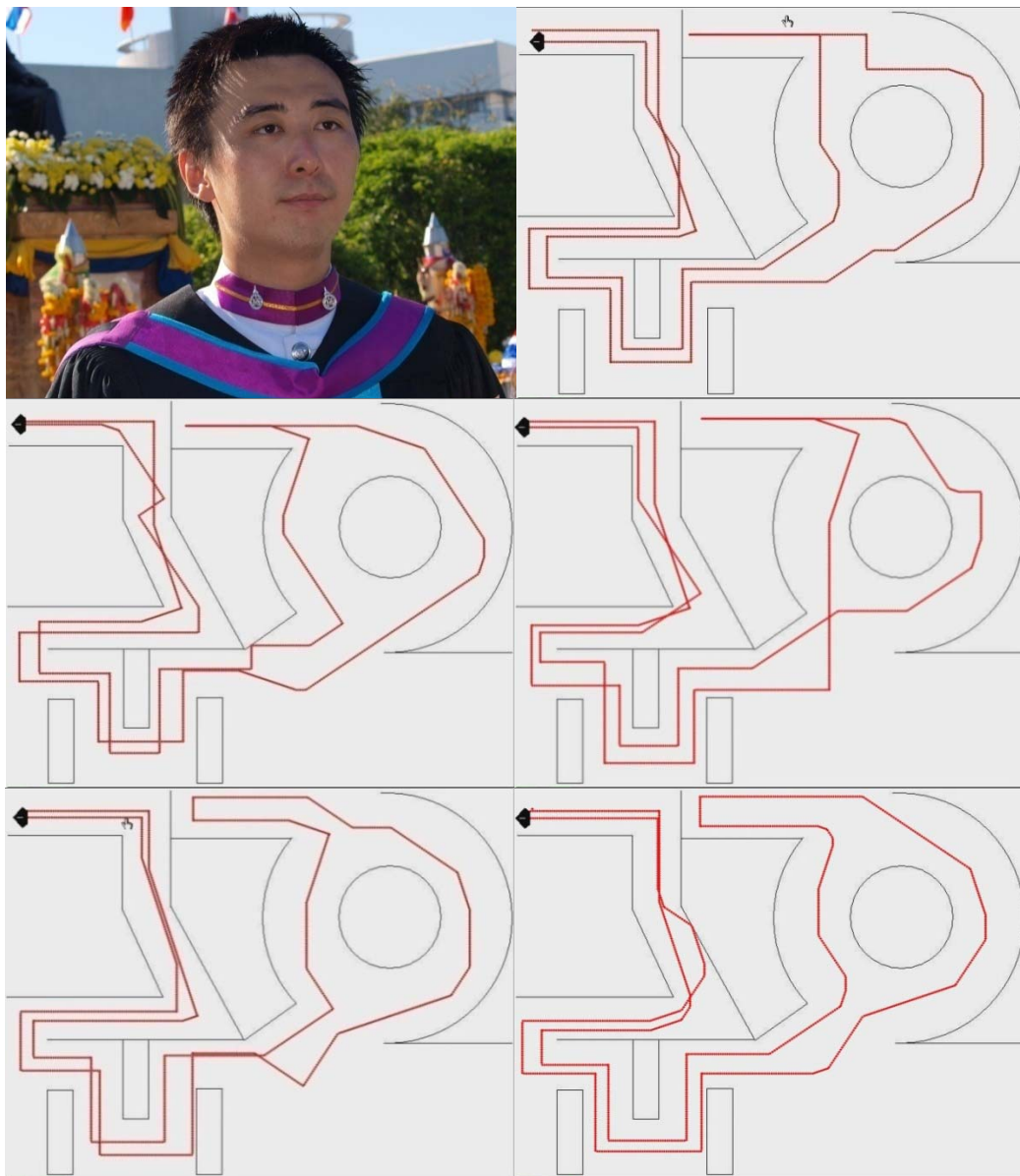


Figure A 4 Mr. Wang Xianwei and his five simulation tracks

Appendix II.5. Mr. Fu Dongjin's test result

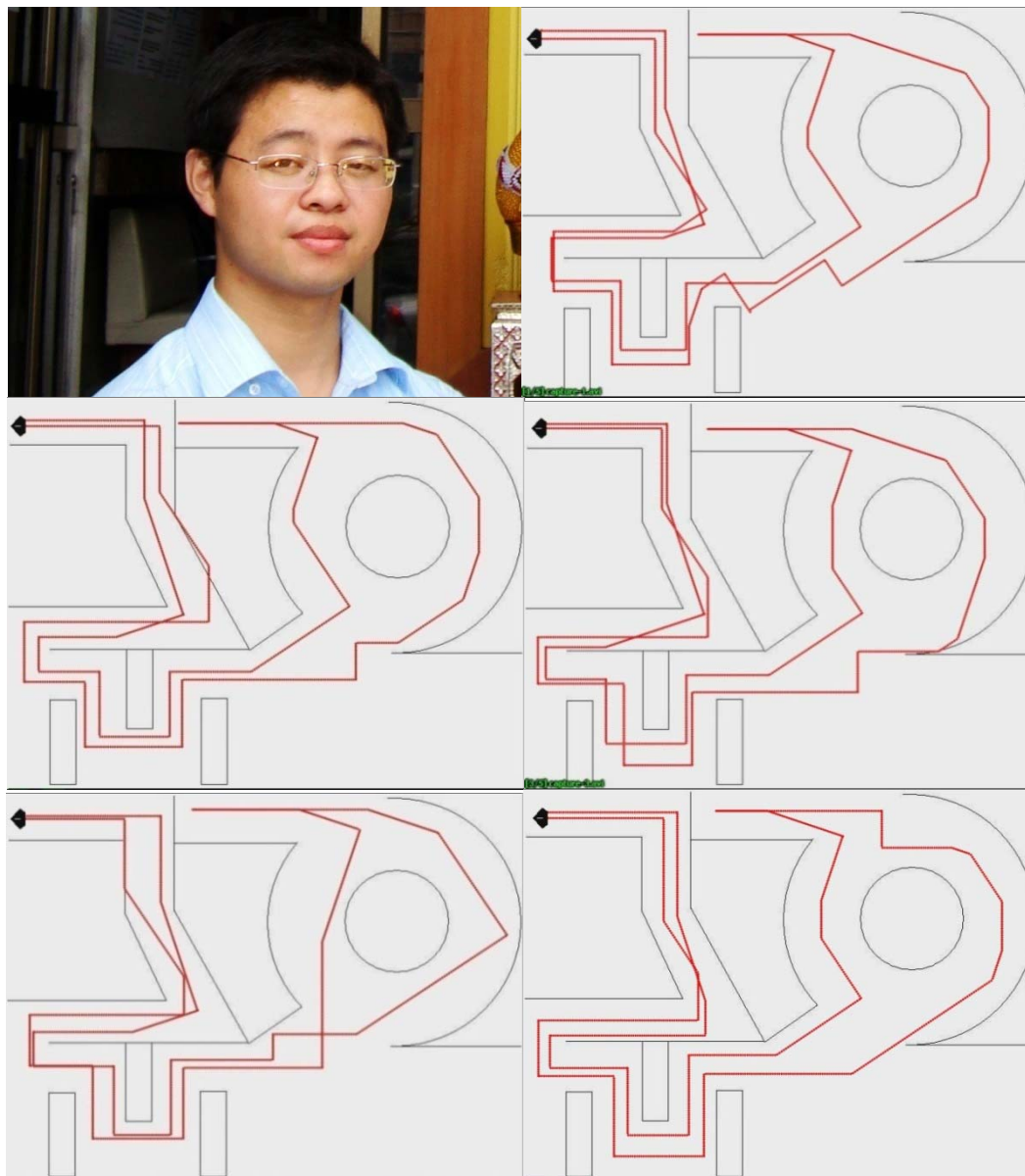


Figure A 5 Mr. Fu Dongjin and his five simulation tracks

Appendix III. HIOKI 3531 Z HITESTER

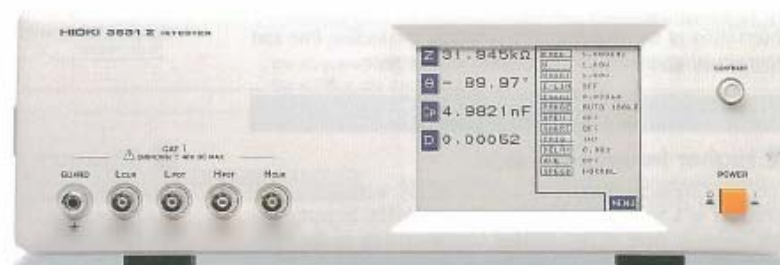
HIOKI

1998

NEW

3522 LCR HiTESTER / 3531 Z HiTESTER

Components measuring instruments



Accuracy $\pm 0.08\%$, frequency range: DC and 1 MHz to 100 kHz (3522) / 42 Hz to 5 MHz (3531)

Impedance meter with a wide test frequency range

CE CE marking relates to EU (European Union) safety regulations, and is required for specified products marketed within the EU. CE marking indicates that the product complies with all of the safety restrictions of relevant EU directives.
* The 3522 and 3531 have been designed to comply with IEC 1010 and EMC standards, in accordance with EU directives.

IEC 1010 International safety standard relating to electrical measurement, control and laboratory equipment. The object of this standard is to lay down conditions to be met by electronic equipment to provide appropriate protection against accident and injury to users, and to specify test procedures for showing that the conditions are met.

EMC Electromagnetic compatibility: when both EMI (electromagnetic interference: emission = not emitting electromagnetic interference) and EMS (electromagnetic susceptibility: immunity = not suffering from effects of electromagnetic interference) measures are taken, this is referred to as electromagnetic compatibility, and means that EMC measures have been taken.

The 3522 LCR HiTESTER and 3531 Z HiTESTER together provide a wide range of test frequencies. The 3522 offers DC and a range from 1 MHz to 100 kHz, and the 3531 covers the range from 42 Hz to 5 MHz. Test conditions can now come closer to a component's operating conditions. The high basic accuracy of $\pm 0.08\%$, combined with ease of use and low price give these impedance meters outstanding cost-performance characteristics.

These will find a wide range of applications, whether for laboratory use for evaluation of operating characteristics, or for production line use, exploiting the full-function interface and comparator functions and rapid response.

Two Models Cover Wide Frequency Range :

3522 LCR HiTESTER

■ Measurement in DC and low frequency ranges

The measurement frequency can be freely set to DC or any value in the 1 mHz to 100 kHz range with four-digit precision. In particular this makes it easy to test sample characteristics in the low frequency range and up to 100 kHz.

■ Fourteen parameters measured

The following parameters can be measured, and selected parameters can be captured by a computer: $|Z|$, $|Y|$, θ , R_p (DCR), R_s (ESR, DCR), G , X , B , L_p , L_s , C_p , C_s , D ($\tan \delta$), and Q .

■ Minimum measurement time 20 ms

Four sampling rates can be selected: FAST, NORMAL, SLOW, and SLOW2. The minimum measurement time of 20 ms (displaying $|Z|$) gives rapid sampling for improved production line efficiency.

(The measurement frequency range varies from one parameter to another.)

■ Enlarged display function

Up to four parameters can be displayed enlarged, for easy observation of the measurement values in production line and other situations where the unit is read at a distance.

■ Memory for thirty sets of measurement conditions

Up to thirty sets of measurement conditions, including comparator values, provide rapid response to constantly changing components on flexible production lines. With multiple measurement conditions in memory, up to five different measurements can be made sequentially. The comparator function lets a single unit provide the logical AND result for this sequence of tests.

■ DC resistance measurement

DC resistance measurement is another feature of the 3522. A single unit, the 3522 can provide the crucial parameters of inductance (L) and DC resistance (DCR) for a transformer or coil.

■ Correlation correction function

The constants a and b can be set in the following correction function expression:

$$\text{Corrected value} = a \times \text{measurement value} + b$$

■ Printer output

With the optional 9442 PRINTER, measurement values, comparator results, and screen printouts can be obtained.

3531 Z HiTESTER

■ Higher frequency range

The measurement frequency can be freely with four-digit precision in a wide range from 42 Hz to 5 MHz. In particular this makes it easy to test sample characteristics in the high frequency range.

■ Fourteen parameters measured

The following parameters can be measured: $|Z|$, $|Y|$, θ , R_p , R_s (ESR), G , X , B , L_p , L_s , C_p , C_s , D ($\tan \delta$), and Q .

■ Minimum measurement time 50 ms

Four sampling rates can be selected: FAST, NORMAL, SLOW, and SLOW2. The minimum measurement time of 50 ms (displaying $|Z|$) gives rapid sampling for improved production line efficiency.

■ Memory for five sets of measurement conditions

Up to five sets of measurement conditions, including comparator values, provide rapid response to constantly changing components on flexible production lines.

As with the 3522, up to five comparator results can be obtained sequentially.

Common features

■ High resolution and high accuracy

The measurement resolution provides a full five digits, and the basic measurement accuracy is $\pm 0.08\%$.

■ Simultaneous setting and measurement

Measurement frequency, measurement signal level, and other measurement conditions can be changed while monitoring the measurement results, enabling effective trial measurements and setting of evaluation conditions.

■ Interactive touch panel operation

Operation is extremely simple: touch the item on the screen to be changed, and the possible settings appear in sequence. The neat and simple front panel eliminates all key switches, for a clutter-free design.

■ Wide setting range for measurement voltage and current

In addition to normal open-loop signal generation, these units provide for voltage/current dependent evaluation, in constant voltage and constant current modes. The signal levels can be set over wide ranges, from 10 mV to 5 Vrms, and from 10 μ A to 100 mA (up to 1 MHz).

■ Four simultaneous measurement items

Any four of the parameters can be chosen for measurement and display.

■ DC bias measurement

Using the optional 9268/9269 DC BIAS UNIT, voltage and current bias measurements are simple. The maximum applied bias is ± 40 V DC, but depends on the measurement conditions.

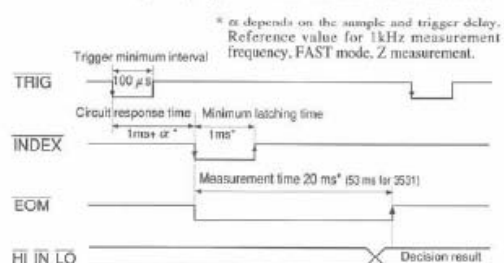
DC, 1 mHz to 100 kHz, and 42 Hz to 5 MHz

External I/O interface

The EXT. I/O connector can input trigger signals, and provides a key lock on/off function, and remote control of the measurement condition loading. Output signals include comparator results and measurement completed signals, for complete line automation.

Timing chart for EXT. I/O sequencing

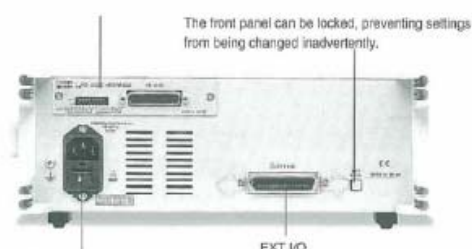
The following chart shows the timing sequence of the trigger (TRIG), analog measurement completion (INDEX), and end-of-measurement (EOM) signals from the EXT. I/O connector.



EXT. I/O signals

- Outputs
 - Internal DC power (+5 V output)
 - Comparator result
 - Analog measurement completion
 - End-of-measurement
- Inputs
 - External DC power supply (+5 V to +24 V can be supplied by external device)
 - External trigger signal
 - Key lock on/off function (3531 only)
 - Memory setting selection

Either a GP-IB or RS-232C interface can be fitted (options).



3522 / 3531 specifications

	3522	3531
Measurement parameters	$ Z , Y , \theta, R_p, R_s$ (DCR), R_s (ESR, DCR), G, X, B, C, p, Cs, Lp, Ls, D (tan δ), Q	$ Z , Y , \theta, R_p, R_s$ (ESR), G, X, B, C, p, Cs, Lp, Ls, D (tan δ), Q
Measurement ranges $ Z , R, X$	10.000 m Ω to 200.00 M Ω (depending on measurement frequency and signal levels)	
θ	-180.00° to +180.00°	-180.00° to +180.00°
C	0.3200 pF to 1.0000 F	0.3200 pF to 370.00 mF
L	32.000 nH to 750.00 kH	32.000 nH to 750.00 kH
D	0.00001 to 9.99999	0.00001 to 9.99999
Q	0.01 to 999.99	0.01 to 999.99
$ Y , G, D$	5.0000 nS to 99.999 S	5.0000 nS to 99.999 S
Basic accuracy	Z: $\pm 0.08\%$ rdg. θ : $\pm 0.05^\circ$	
Measurement frequency	DC, 1 mHz to 100 kHz	42 Hz to 5 MHz
Measurement signal levels	10 mV to 5 V rms 10 μ A to 100 mA rms	
Output impedance	50 Ω	
Display screen	LCD with backlight / 99999 (full 5 digits)	
Measurement time (typical values for displaying $ Z $)	FAST: 20ms, NORMAL: 65ms, SLOW 1/2: 140ms / 1040ms	FAST: 50ms, NORMAL: 70ms, SLOW 1/2: 125ms / 200ms
Settings in memory	Maximum 30 sets	Maximum 5 sets
Comparator functions	HI/NI/LO settings for two measurement parameters; percentage or absolute value settings	
DC bias	External DC bias ± 40 V max. (option)	
External printer	9442 PRINTER (option)	—
External interfaces	GP-IB or RS-232C (selectable options), external I/O for sequencer use	
Power source	100, 120, 220 or 240 V ($\pm 10\%$) AC (selectable), 50/60 Hz	
Maximum rated power	40 VA approx.	50 VA approx.

Measurement: All parameter ranges are determined by the $|Z|$ range.
100 m Ω , 1 Ω , 10 Ω , 100 Ω , 1 k Ω , 10 k Ω , 100 k Ω , 1 M Ω , 10 M Ω , 100 M Ω ; (100 M Ω range 3522 only)

Measurement frequency:
[3522] : DC, 1 mHz to 100 kHz ($\pm 0.005\%$)
Up to 10 Hz (1 mHz steps); 10 Hz to 100 Hz (10 mHz); 100 Hz to 1 kHz (100 mHz); 1 kHz to 10 kHz (1 Hz); 10 kHz to 100 kHz (10 Hz)
[3531] : 42 Hz to 5 MHz ($\pm 0.005\%$)
Up to 1 kHz (0.1 Hz steps); 1 kHz to 10 kHz (1 Hz); 10 kHz to 100 kHz (10 Hz); 100 kHz to 1 MHz (100 Hz); 1 MHz to 5 MHz (1 kHz)

Measurement levels:
[Voltage and constant voltage]
10 mV to 5 V rms (DC to 1 MHz)
50 mV to 1 V rms (1 MHz to 5 MHz)
Maximum short-circuit current 100 mA rms
3522: 1 mV steps
3531: 10 mV steps

[Constant current]
10 μ A to 100 mA rms (DC to 1 MHz)
50 μ A to 20 mA rms (1 MHz to 5 MHz)
Maximum voltage 5 V rms
10 μ A rms steps

Dimensions and mass:
3522: 125 (H) \times 313 (W) \times 290 (D) mm; 4.5 kg approx.
3531: 121 (H) \times 352 (W) \times 323 (D) mm; 6.5 kg approx.



Changing Settings During Measurement

Z	1.5702k Ω	FREQ	1.000kHz
θ	-89.58°	V	1.000V
Cs	101.36nF	Vmax1	1.000V
D	0.00733	I-LIM	OFF
		Imax1	0.639mA
		RANGE	AUTO 10k Ω
		OPEN	OFF
		SHORT	OFF
		TRIG	INT
		DELAY	0.00 μ s
		AVE	OFF
		SPEED	NORMAL

MENU

Simple touch panel operation

Setting and changing the test conditions has never been simpler, with this intuitive touch panel. The keys which are active appear in reverse video, and a touch of the item or value to be changed is enough. Moreover, the setting screens also show the measurement values in real time, allowing flexible monitoring while changing test signal settings.

The 3522 also provides an enlarged display for any four parameters, for increased visibility at a distance on production lines.

* The screens show typical examples on the 3522.

Initial screen
Shows measurement values for any selected four parameters, and current settings of conditions.

Z	1.5702k Ω	Z	Y	θ
		Cs	Cp	D
		Rs	G	Rp
		X	B	OFF

* SET PARAMETER *

Parameter setting screen
Select any four of the parameters for display.

Z	1.5702k Ω	FREQ	LEVEL	LIMIT
θ	-89.58°	RANGE	OPEN	SHORT
Cs	101.36nF	TRIG	DELAY	AVE
D	0.00733	SPEED		

* SELECT MENU *

Menu screen
Select an item, and switch to the corresponding setting screen.

Z	1.5702k Ω	APPLICATION MENU		
θ	-89.58°	COMP	SCALE	CONT
Cs	101.36nF	ON	ON	REARS
D	0.00733	LOAD	SAVE	
		RESET		

* SELECT MENU *

Application menu
Save and load measurement conditions, and set comparator execution, enlarged display, and so on.

Z	1.5702k Ω	7	8	9
θ	-89.58°	4	5	6
Cs	101.36nF	1	2	3
D	0.00700	0	.	-

* SET FREQ *

Z	1.5702k Ω	* SET LEVEL *		
θ	-89.58°	FREQ	1.000kHz	
Cs	101.36nF	V	1.000V	
D	0.00733	Vmax1	1.000V	

Measurement frequency and level setting screens
Use the numeric keypad or digit keys to enter the setting values, changing the test frequency or level while monitoring the measurement. The level setting can be open-circuit voltage, constant voltage, or constant current.

Z	1.5702k Ω		
θ	-89.58°		
Cs	101.36nF		
D	0.00733		

* CONTINUOUS MEAS *

Enlarged display and comparator setting screens
Set the enlarged display or select the settings saved in memory to execute continuous measurement.

Personal computer link

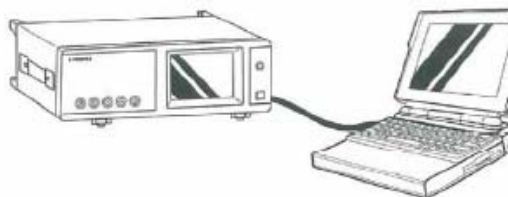
Effective Analysis and Processing of Measurement Data

External control by computer

By installing the optional 9593-01, RS-232C INTERFACE or 9518-01 GP-IB INTERFACE, all of the 3522/3531 functions other than power on/off can be controlled from a computer.

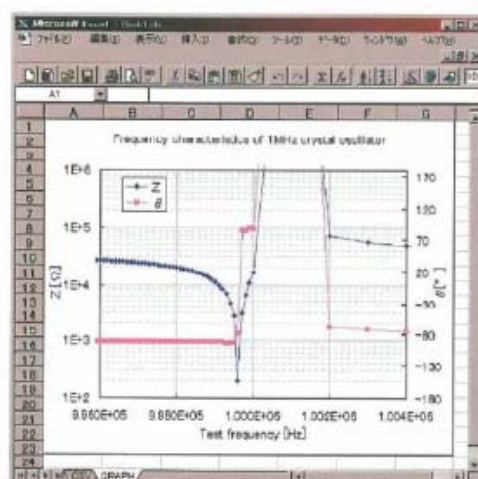
Graphing with a spreadsheet program

Measurement data captured by a personal computer can be displayed graphically by using standard spreadsheet software. The example below uses the provision for continuously varying frequency to capture the frequency characteristics for a 1 MHz quartz oscillator measured



with the 3531 into Excel*, then presents the results graphically. The four-digit resolution for the frequency allows the characteristics of the steep resonance peak to be shown on the graph.

* Excel is a registered trademark of Microsoft.



9593-01, RS-232C INTERFACE specification

Transmission method : Start-stop asynchronous
 Transmission rates : 2400, 4800, 9600 and 19200 baud (3522)
 1200, 2400, 4800 and 9600 baud (3531)
 Data bits : 7 or 8
 Parity : Odd, even or none
 Stop bits : 1, 1.5 or 2

Delimiter : CR+LF, LF
 Flow control : XON/XOFF, hardware (3522 : hardware only)
 (According to DIP switch setting)
 Connection : D-sub 25-pin, male/male connector,
 reverse connection

9442 PRINTER (3522 only)



The optional 9442 PRINTER allows measurement results and screen copies to be printed. This is convenient for permanent records of inspections and so forth.

(Connection requires the optional 9593-01 RS-232C INTERFACE, 9446 CONNECTION CABLE, and AC ADAPTER.)

Example of printing

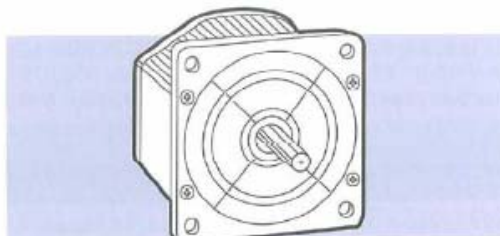
Cs 984.15n F	D	0.00017	
Cs 984.14n F	D	0.00017	
Cs 984.10n F	D	0.00017	
Cs 984.20n F	D	0.00034	
Cs 983.91n F	L0	D	0.00052 HI
Cs 983.89n F	L0	D	0.00034 IN
Cs 984.03n F	IN	D	0.00017 L0
Cs 983.89n F	L0	D	0.00052 HI
Cs 983.95n F	L0	D	0.00034 IN
Cs 983.95n F	L0	D	0.00052 HI

Flexible Measurement Signals Widen Scope for Application

Applications

■ Evaluation of signal-dependent components

Since any test signal can be selected, it is possible to measure the inductance of winding, floating capacitance, characteristics at operating frequency, and low frequency resistance components. The 3522 further allows inductance (L) and DC resistance (DCR) to be measured by the same unit.



Example of measuring signal dependence of coils

For chokes, transformers, and other components with an inductive core, the values depend on the measurement signal. By varying the measurement current, measurements showing the signal dependence of the coil can be shown as a graph.

The 3522 and 3531 provide three modes for selecting the measurement signal according to the component characteristics: open-circuit voltage (V), constant voltage (CV), or constant current (CC).

V mode : set V_0

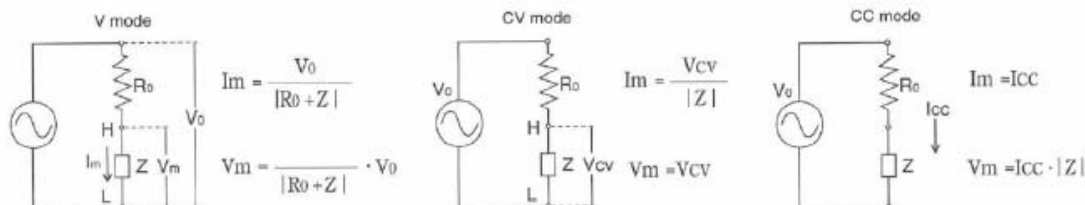
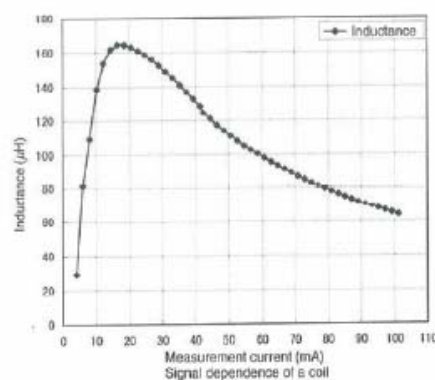
CV mode : set V_0 so that the voltage across the component is the CV value (V_{cv})

CC mode : set V_0 so that the current through the component is the CC value (I_{cc})

V_m : voltage monitor value

I_m : current monitor value

R₀ : output impedance (50Ω constant)



Evaluating battery characteristics by measuring the internal resistance

By measuring the internal resistance of lead-acid or compact storage batteries, the state of deterioration of the battery, and its lifetime and characteristics can be determined.

In particular, the 3522 provides low-frequency measurement from 1 mHz, allowing low frequency electrochemical impedance measurement, and other applications in basic chemical research.

Measurement values:

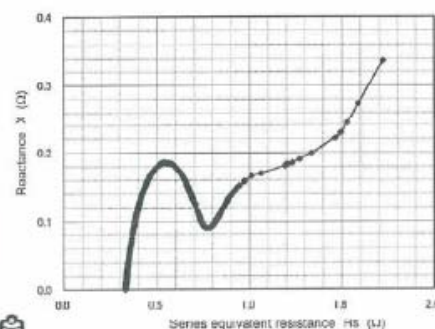
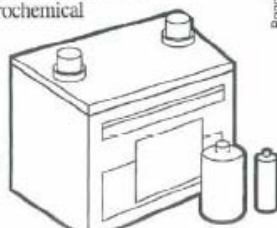
R_s (DCR), R_s, |Z|, θ, etc.

Measurement frequency:

DC, 1 kHz fixed, and variable frequency

Measurement signal:

constant current (CC) mode



Frequency characteristics of a manganese battery (1 mHz to 100 kHz)
[cole-cole plot]

Measurement accuracy and ranges *

Conditions : temperature range 23 °C ±5 °C, 80% RH or less (no condensation)

After 60-minute warm-up from powering on, and open-circuit and short-circuit correction.

Using the 9262 TEST FIXTURE, and measurement signal levels 1.001 V to 5.000 V (3522), 0.46 V to 1.00 V (3531); measurement speed SLOW2.

* Measurement ranges and accuracy depend on the test fixture used, the measurement signal levels, and the measurement speed.

3522 Accuracy

Range	Impedance	DC	1m to 99.99Hz	100.0 to 999.9Hz	1.000k to 10.00kHz	10.01k to 100.0kHz
100MΩ	200MΩ	A=1 B=1	A=7 B=5	A=4.5 B=1	A=4.5 B=1	
	10MΩ		A=4 B=3	A=3 B=1.5	A=2.5 B=1.5	
10MΩ	10MΩ	A=0.5 B=0.3	A=2 B=0.5	A=0.7 B=0.4	A=0.7 B=0.4	A=1.5 B=0.5
	1MΩ		A=1 B=0.2	A=0.7 B=0.2	A=0.5 B=0.2	A=2 B=0.3
1MΩ	1MΩ	A=0.2 B=0.05	A=0.7 B=0.03	A=0.25 B=0.03	A=0.2 B=0.03	A=0.7 B=0.03
	100kΩ		A=0.35 B=0.02	A=0.15 B=0.02	A=0.1 B=0.02	A=0.5 B=0.1
100kΩ	100kΩ	A=0.1 B=0.01	A=0.4 B=0.01	A=0.2 B=0.002	A=0.15 B=0.002	A=0.35 B=0.01
	10kΩ		A=0.28 B=0.002	A=0.12 B=0.002	A=0.08 B=0.002	A=0.1 B=0.02
10kΩ	10kΩ	A=0.1 B=0.01	A=0.38 B=0.002	A=0.15 B=0.002	A=0.1 B=0.002	A=0.2 B=0.002
	1kΩ		A=0.25 B=0.001	A=0.1 B=0.001	A=0.05 B=0.001	A=0.08 B=0.002
1kΩ	1kΩ	A=0.1 B=0.01	A=0.36 B=0.001	A=0.12 B=0.001	A=0.08 B=0.001	A=0.15 B=0.001
	100Ω		A=0.25 B=0.001	A=0.1 B=0.001	A=0.05 B=0.001	A=0.08 B=0.002
100Ω	100Ω	A=0.1 B=0.02	A=0.36 B=0.01	A=0.15 B=0.01	A=0.15 B=0.01	A=0.15 B=0.02
	10Ω		A=0.25 B=0.005	A=0.1 B=0.005	A=0.05 B=0.005	A=0.08 B=0.01
10Ω	10Ω	A=0.2 B=0.05	A=0.5 B=0.04	A=0.25 B=0.02	A=0.25 B=0.01	A=0.35 B=0.02
	1Ω		A=0.35 B=0.02	A=0.2 B=0.01	A=0.15 B=0.01	A=0.2 B=0.02
1Ω	1Ω	A=0.3 B=0.3	A=1 B=0.6	A=0.5 B=0.3	A=0.35 B=0.2	A=0.7 B=0.3
	100mΩ		A=0.6 B=0.4	A=0.35 B=0.2	A=0.3 B=0.1	A=0.45 B=0.1
100mΩ	100mΩ	A=1 B=0.5	A=7 B=4	A=3.5 B=1.5	A=2.5 B=1.5	A=3.5 B=1.5
	10mΩ		A=5 B=2	A=2.5 B=1	A=1.5 B=1	A=2 B=1

Upper figure A ... basic accuracy for |Z| (±% rdg.)
Lower figure A ... basic accuracy for θ (±deg.)
B is coefficient for sample impedance

When DC resistance measurement,
A is accuracy for R (±% rdg.)
B is coefficient for sample resistance

The expression for calculating accuracy is different in the ranges above 1 kΩ and below 100 Ω.
For details refer to the following expressions.

Range 1 kΩ and above...
Accuracy = $A + \frac{B \times |range - Z_x| \times 10}{Range}$

Range 100 Ω and below...
Accuracy = $A + \frac{B \times |range - Z_x| \times 10}{Range}$

Z_x is the measured impedance of the sample (|Z|).

3531 Accuracy

Range	Impedance	42 Hz and up	100 Hz and up	1.001 kHz and up	10.01 kHz and up	100.1 kHz and up	1.001 MHz to 5 MHz			
10MΩ	200MΩ	A=0.5 B=0.3		A=0.4 B=0.15	A=2 B=0.5					
	10MΩ							A=0.3 B=0.2	A=0.3 B=0.15	A=2 B=0.5
	1MΩ									
1MΩ	1MΩ	A=0.2 B=0.05		A=0.15 B=0.05	A=0.2 B=0.08	A=3 B=2.5				
	100kΩ							A=0.1 B=0.02	A=0.2 B=0.02	A=0.25 B=0.08
100kΩ	100kΩ	A=0.15 B=0.01	A=0.08 B=0.01	A=0.15 B=0.01	A=0.15 B=0.05	A=0.2 B=0.08	A=2 B=0.5			
	10kΩ							A=0.08 B=0.005	A=0.08 B=0.005	A=0.15 B=0.01
10kΩ	10kΩ	A=0.15 B=0.01	A=0.08 B=0.01	A=0.08 B=0.01	A=0.08 B=0.03	A=0.2 B=0.05	A=1 B=0.4			
	1kΩ							A=0.1 B=0.005	A=0.08 B=0.005	A=0.05 B=0.005
1kΩ	1kΩ	A=0.15 B=0.01	A=0.08 B=0.01	A=0.08 B=0.01	A=0.08 B=0.03	A=0.2 B=0.05	A=1 B=0.4			
	100Ω							A=0.1 B=0.005	A=0.08 B=0.005	A=0.05 B=0.005
100Ω	100Ω	A=0.15 B=0.02	A=0.08 B=0.02	A=0.15 B=0.02	A=0.15 B=0.02	A=0.25 B=0.02	A=0.8 B=0.02			
	10Ω							A=0.1 B=0.01	A=0.08 B=0.01	A=0.08 B=0.01
10Ω	10Ω	A=0.2 B=0.05	A=0.2 B=0.04	A=0.2 B=0.04	A=0.4 B=0.1	A=1.5 B=1.5				
	1Ω							A=0.15 B=0.03	A=0.1 B=0.03	A=0.4 B=0.1
1Ω	1Ω	A=0.6 B=0.4	A=0.5 B=0.4	A=0.5 B=0.4	A=1.5 B=1.5	A=1 B=1				
	100mΩ							A=0.5 B=0.3	A=0.5 B=0.2	A=1.5 B=1.5
100mΩ	100mΩ	A=5 B=5	A=5 B=4	A=5 B=5	A=5 B=5					
	10mΩ							A=5 B=3	A=5 B=2	A=5 B=3

Method of determining accuracy

- The measurement accuracy can be calculated from the impedance of the sample, the measurement range, the measurement frequency, and the basic accuracy A and coefficient B from the above tables.
- The expression for calculating accuracy is different in the ranges above 1 kΩ and below 100 Ω.
- For C and L, find the basic accuracy A and coefficient B either by direct measurement of the impedance or by approximate calculation as follows.

$$|Z_x(\Omega)| \approx \omega L(\text{H}) \quad (\theta \approx 90^\circ)$$

$$\approx \frac{1}{\omega C(\text{F})} \quad (\theta \approx -90^\circ)$$

$$\approx R(\Omega) \quad (\theta \approx 0^\circ)$$

Example calculation (The value A and B for the 3522)

Sample impedance Z_x: 500 Ω (measured)

Measurement conditions: frequency 10 kHz, signal level 2 V, range 1 kΩ

From table above, basic Z accuracy A = 0.08, coefficient B = 0.001. Inserting these in the calculation expression yields:

$$Z \text{ accuracy} = 0.08 + \frac{0.001 \times |10 \times 5 \times 10^3 - 10^3|}{10^3} = 0.084 (\pm\% \text{rdg.})$$

Similarly for θ basic accuracy A = 0.08, coefficient B = 0.001, and thus:

$$\theta \text{ accuracy} = 0.05 + \frac{0.001 \times |10 \times 5 \times 10^3 - 10^3|}{10^3} = 0.054 (\pm\% \text{deg.})$$

Options for a wide range of applications



9140 FOUR-TERMINAL PROBE

DC to 100 kHz

9143 PINCHER PROBE

DC to 5 MHz

9261 TEST FIXTURE

DC to 5 MHz

9262 TEST FIXTURE

DC to 5 MHz

9263 SMD TEST FIXTURE

DC to 5 MHz

* All cable lengths are 1 m.



9268 DC BIAS VOLTAGE UNIT

Maximum applied voltage: ± 40 V DC

9269 DC BIAS CURRENT UNIT

Maximum applied current: ± 2 A DC

Bias unit attached

9442 PRINTER



9443 AC ADAPTER



9443-02 (for EU) 9443-01 (for Japan)

Printing method : Thermal serial dot printer
 Recording width : 112mm
 Printing speed : 52.5cps
 Power supply : 9443 AC ADAPTER or supplied nickel-hydrogen battery pack (prints 3000 lines on full charge from 9443)

Approx. dimensions : 160 (W) \times 66.5 (H) \times 170 (D), 580 g and weight

* Connecting the 9442 PRINTER requires the optional 9593-01 RS-232C INTERFACE, 9446 CONNECTION CABLE, and AC ADAPTER.

3522 LCR HITESTER

3531 Z HITESTER

(Standard accessories: power cord, 3-pin/2-pin power adapter, spare power fuse (1 A for 100/120 V rating, 0.5 A for 220/240 V rating))

Test fixtures are not supplied with the unit.
 Select an optional test fixture when ordering.

Optional accessories

9140 FOUR-TERMINAL PROBE

9143 PINCHER PROBE

9261 TEST FIXTURE

9262 TEST FIXTURE (direct connection type)

9263 SMD TEST FIXTURE (direct connection type)

9268 DC BIAS VOLTAGE UNIT

9269 DC BIAS CURRENT UNIT

9165 CONNECTION CORD (for 9268/9269; BNC to BNC; 1.5 m)

9166 CONNECTION CORD (for 9268/9269; BNC to clips; 1.5 m)

9593-01 RS-232C INTERFACE

9518-01 GP-IB INTERFACE

9151-02 GP-IB CONNECTION CABLE (2 m)

9151-04 GP-IB CONNECTION CABLE (4 m)

9442 PRINTER (for 3522)

9443-01 AC ADAPTER (for printer, Japan)

9443-02 AC ADAPTER (for printer, EU)

9443-03 AC ADAPTER (for printer, America)

9446 CONNECTION CABLE (for printer)

1196 RECORDING PAPER (25 m, 10 rolls)

HIOKI

HIOKI E. E. CORPORATION

DISTRIBUTED BY

HEAD OFFICE:

81 Kozumi, Ueda, Nagano, 386-11, Japan
 FAX: 0268-28-0568 / TEL: 0268-28-0562
 E-mail: os-com@hioki.co.jp

Internet HIOKI web-page <http://www.hioki.co.jp/>

All information correct as of Dec 25, 1997. All specifications are subject to change without notice.

F3522E1-72E-05K Printed in Japan

VITAE

Name Mr. Huang Yunfei

Student ID 5010120154

Educational Attainment

Degree	Name of Institution	Year of Graduation
Bachelor of Electrical Engineering	JiangXi University of Science and Technology	2007

List of Publication and Proceedings

- [1] Y. F. Huang, P. Phukpattaranont, B. Wongkittisuksa, and S. Tanthanuch, “Development of a bioimpedance-based human machine interface for wheelchair control,” *Proceedings of the ECTI International Conference (ECTI-CON 2009)*, pp. 1032–1035, Pattaya, Thailand, May 2009.
- [2] Y. F. Huang, P. Phukpattaranont, B. Wongkittisuksa, and S. Tanthanuch, “A Novel Design and Development on Bioimpedance-Based Wheelchair Control,” *Proceedings of the 3rd International Convention on Rehabilitation Engineering & Assistive Technology (i-CREATE 2009)*, pp. 17–20, Singapore, April 2009.
- [3] Y. F. Huang, P. Phukpattaranont, S. Tanthanuch, K. Chetpatananondh, B. Wongkittisuksa, and C. Limsakul, “Evaluation of Human Machine Interface for Wheelchair Control with Bioimpedance,” *Proceedings of the 24th Japanese Conference on the Advancement of Assistive and Rehabilitation Technology (the 24th JCAART)*, pp. 227–228, Japan, August 2009.